



# *Institute of Paper Science and Technology*

**IMPULSE DRYING PERFORMANCE DATABASE FOR HEAVY WEIGHT GRADES OF PAPER**

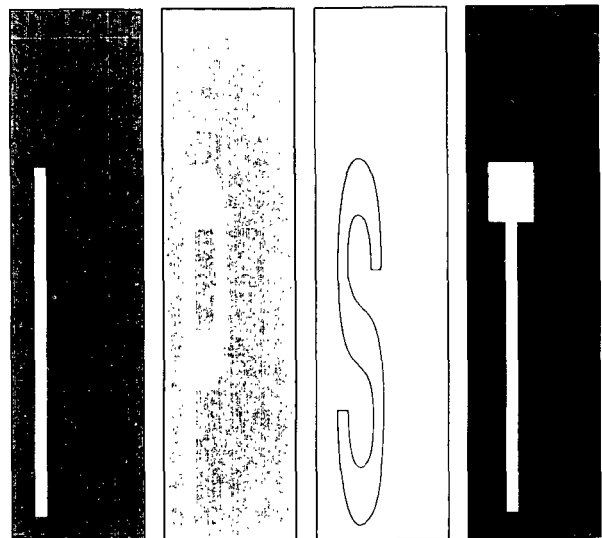
**Project 3753**

**Report 1**

**to the**

**TECHNICAL DIVISION OF THE CONTAINERBOARD AND KRAFT PAPER GROUP  
OF  
THE AMERICAN PAPER INSTITUTE**

**December 31, 1992**



*Atlanta, Georgia*

INSTITUTE OF PAPER SCIENCE AND TECHNOLOGY  
PURPOSE AND MISSION STATEMENT

The Institute of Paper Science and Technology is a unique organization whose charitable, educational, and scientific purpose evolves from the singular relationship between the Institute and the pulp and paper industry which has existed since 1929. The purpose of the Institute is fulfilled through three missions, which are:

- to provide high quality students with a multidisciplinary graduate educational experience which is of the highest standard of excellence recognized by the national academic community and which enables them to perform to their maximum potential in a society with a technological base; and
- to sustain an international position of leadership in dynamic scientific research which is participated in by both students and faculty and which is focused on areas of significance to the pulp and paper industry; and
- to contribute to the economic and technical well-being of the nation through innovative educational, informational, and technical services.

ACCREDITATION

The Institute of Paper Science and Technology is accredited by the Commission on Colleges of the Southern Association of Colleges and Schools to award the Master of Science and Doctor of Philosophy degrees.

NOTICE AND DISCLAIMER

The Institute of Paper Science and Technology (IPST) has provided a high standard of professional service and has put forth its best efforts within the time and funds available for this project. The information and conclusions are advisory and are intended only for internal use by any company who may receive this report. Each company must decide for itself the best approach to solving any problems it may have and how, or whether, this reported information should be considered in its approach.

IPST does not recommend particular products, procedures, materials, or service. These are included only in the interest of completeness within a laboratory context and budgetary constraint. Actual products, procedures, materials, and services used may differ and are peculiar to the operations of each company.

In no event shall IPST or its employees and agents have any obligation or liability for damages including, but not limited to, consequential damages arising out of or in connection with any company's use of or inability to use the reported information. IPST provides no warranty or guaranty of results.

The Institute of Paper Science and Technology assures equal opportunity to all qualified persons without regard to race, color, religion, sex, national origin, age, handicap, marital status, or Vietnam era veterans status in the admission to, participation in, treatment of, or employment in the programs and activities which the Institute operates.

INSTITUTE OF PAPER SCIENCE AND TECHNOLOGY

Atlanta, Georgia

IMPULSE DRYING PERFORMANCE DATABASE FOR HEAVY WEIGHT GRADES OF PAPER

Project 3753

Report 1

A Progress Report

to the

TECHNICAL DIVISION OF THE CONTAINERBOARD AND KRAFT PAPER GROUP  
OF  
THE AMERICAN PAPER INSTITUTE

By

David I. Orloff

December 31, 1992

## TABLE OF CONTENTS

SUMMARY.....	1
OVERVIEW AND OBJECTIVES.....	2
EXPERIMENTAL METHODS.....	4
Formation of Oriented Sheets on the Formette Dynamique.....	4
Measurement of Fiber Dimensions.....	4
Hydrodynamic Specific Surface Measurements.....	6
Double-felted Pressing and Impulse Drying Simulation.....	8
RESULTS.....	9
Hydrodynamic Specific Surface.....	9
Critical Temperature.....	10
Impulse Dying vs. Double-felted Pressing.....	12
CONCLUSIONS.....	19
RECOMMENDATIONS.....	19
REFERENCES.....	20
ACKNOWLEDGMENTS.....	21
APPENDIX.....	22

The first year's work of this two-year study has demonstrated that multi-ply linerboard having significant concentrations of recycle fiber can be successfully impulse dried.

In the second year, the laboratory-scale database will be extended to include three-ply sheets and furnishes composed of blends of Douglas fir and recycled fiber. In addition, the results of the first year will be confirmed in batch pilot-scale experiments.

### OVERVIEW AND OBJECTIVES

Ongoing laboratory and pilot-scale research at the Institute of Paper Science and Technology (IPST) has demonstrated that heavy weight grades of paper, such as linerboard, can be successfully impulse dried (1-15). That research has shown that deleterious sheet delamination can be avoided by a combination of processing strategies. These strategies include steps to make the prepressed sheets highly permeable to water flow and steps to reduce excess heat transfer to the sheet that results in excessive internal flash evaporation at the exit of the impulse dryer.

Research at IPST suggests that high sheet darcian permeability (low hydrodynamic specific surface) can be obtained by limiting refining to the minimum required for product aesthetics and by prepressing the sheet to as high a solids as possible. In addition, IPST research suggests that excessive pressure dependent heat transfer can be eliminated by using press roll surfaces composed of materials having low thermal conductivity, low heat capacity, and low density.

Previous IPST research was conducted with single-ply linerboard sheets composed of virgin southern pine that was minimally refined to eliminate shives. In contrast, commercial linerboard is usually two or three ply and composed of blends of virgin Kraft and recycled fiber. While current recycle content varies from mill to mill, there is increasing environmental pressure to increase recycle content. Mills in the U.S. typically use recycled fiber from old corrugated containers which are collected at warehouses and other high volume locations. In current practice, the amount of recycled fiber included in linerboard is limited by the fact that sheet strength properties decrease when recycle content is increased. Recycled fiber has the additional disadvantage in that it has a poor physical appearance. To improve the appearance of liner made with recycle fiber, U.S. manufacturers typically form a multi-ply sheet where the recycled fiber is contained in a bottom or inner layer, and outer layers are made from virgin Kraft sufficiently refined to impart a good appearance to the product.

The present research was designed to extend impulse drying to sheet constructions that correspond to commercial sheet structures. The experimental program was conducted in three experimental groups based on the sheet structure as shown in Figure 1.

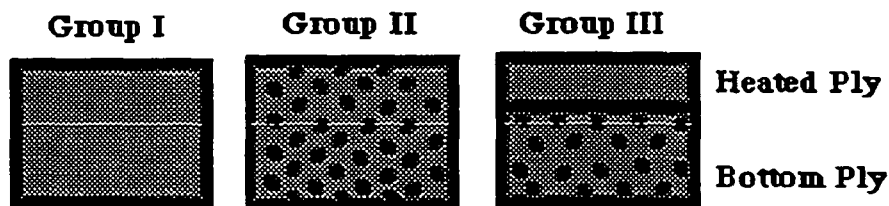


Figure 1. Schematic of Sheet Structures.

## SUMMARY

Laboratory-scale impulse drying simulations have been conducted to identify important pulp substitution variables and quantify the benefit of impulse drying for multi-ply linerboard manufactured with recycled furnishes. In the first year of this two-year study, impulse drying simulations have been performed on one and two layer handsheets formed on the Formette Dynamique. The experiments were conducted in three consecutive experimental groups.

Preliminary experiments identified procedures for operating the Formette Dynamique to achieve commercial orientation and to map out the influence of refining on fiber morphology and sheet permeability for the range of furnishes to be evaluated in the experimental program. The major result of these preliminary experiments was to show that Z-directional permeability was nearly independent of fiber orientation in the sheet while being strongly dependent on refining. In particular, the refining effect on permeability was found to be species dependent. For example, at high freeness, Douglas fir was less permeable to water transport than was southern pine.

In the first experimental group, single-ply 42 lb liner made from five minimally refined furnishes was impulse dried to explore the influence of fiber species and lignin content on impulse drying. High and low Kappa southern pine and Douglas fir were evaluated, as was a OCC furnish. The major conclusions of this part of the work were that Kappa number had little effect on impulse drying performance, while southern pine was found to have an advantage over Douglas fir. As a result of southern pine yielding less fines at a given refining level, southern pine could be impulse dried at higher temperatures resulting in higher outgoing dryness and enhanced physical properties.

The second group of experiments was designed to answer the question of how much recycled fiber could be blended with virgin Kraft and still be successfully impulse dried. Here, the criterion for success was that the strength and dryness imparted by impulse drying be superior to that which could be achieved by conventional double-felted pressing at the same impulse as used during impulse drying. In these experiments, single-ply sheets were formed from blends of OCC refined to two different freenesses, with a lightly refined virgin southern pine. Southern pine was chosen based on the results of the first group of experiments. The general conclusion of the second group of experiments was that the strength advantage of impulse drying was observed at recycle concentrations of 50 percent or less, while a dryness advantage was observed for blends having recycle concentrations of 75 percent or less.

In the third group of experiments, two-ply sheets of various constructions were impulse dried to determine how the composition of the top and bottom layer influence optimum impulse drying operating conditions and resulting dryness and physical properties. The major conclusion was that the composition of that part of the sheet in contact with the heated surface controls the critical impulse drying temperature. The critical impulse drying temperature is defined as the temperature above which sheet delamination occurs. When the bottom sheet was composed of 50 percent virgin southern pine Kraft and 50 percent recycled fiber, superior impulse drying dryness and physical property development were observed for top sheet compositions having freenesses of 450 ml CSF or more. Sheets constructed with a bottom sheet of recycled fiber and a top sheet of virgin southern pine Kraft showed enhanced dryness and strength as long as the heated surface of the sheet had a freeness of 600 ml CSF or more.

Table 1 shows the composition of sheets in each of these groupings. In the first grouping, pulp species and pulp Kappa number were investigated as relevant variables. In the second grouping, blends of virgin and recycled OCC were investigated. While in the third group of experiments, the influence of the composition and freeness of both heated and bottom plies were investigated. In all cases, the total basis weight of the sheets was kept at 205 g/m<sup>2</sup>.

Table 1. Sheet Composition.

Group	Heated Ply				Bottom Ply			
	Wt. % of Total	Species or Type	Kappa No.	Freeness ml CSF	Wt. % of Total	Species or Type	Kappa No.	Freeness ml CSF
I	100	D. Fir	HIGH	HIGH	-----	-----	-----	-----
	100	D. Fir	LOW	HIGH	-----	-----	-----	-----
	100	S. Pine	HIGH	HIGH	-----	-----	-----	-----
	100	S. Pine	LOW	HIGH	-----	-----	-----	-----
	100	OCC	HIGH	HIGH	-----	-----	-----	-----
	100	OCC	HIGH	LOW	-----	-----	-----	-----
II	25	S.Pine	HIGH	HIGH	-----	-----	-----	-----
	75	OCC	HIGH	HIGH	-----	-----	-----	-----
	50	S.Pine	HIGH	HIGH	-----	-----	-----	-----
	50	OCC	HIGH	HIGH	-----	-----	-----	-----
	75	S.Pine	HIGH	HIGH	-----	-----	-----	-----
	25	OCC	HIGH	HIGH	-----	-----	-----	-----
III	20	S. Pine	HIGH	HIGH	40	S.Pine	HIGH	HIGH
					40	OCC	HIGH	HIGH
	20	S. Pine	HIGH	MED	40	S.Pine	HIGH	HIGH
					40	OCC	HIGH	HIGH
	20	S. Pine	HIGH	LOW	40	S.Pine	HIGH	HIGH
					40	OCC	HIGH	HIGH
	20	S. Pine	HIGH	HIGH	80	OCC	HIGH	HIGH
	20	S. Pine	HIGH	LOW	80	OCC	HIGH	HIGH

In previous research, sheet delamination has been shown to begin at a critical temperature that depends on the hydrodynamic specific surface of the sheet to be impulse dried. Hydrodynamic specific surface, in turn, is expected to be a function of fiber dimensions and extent of prepressing (10). Therefore, for each of the sheet compositions listed in Table 1, fiber dimensions and hydrodynamic specific surface were determined from sheet samples with the intent that these measurements would be useful in predicting critical temperature.

## EXPERIMENTAL METHODS

### Formation of Oriented Sheets on the Formette Dynamique

The Formette Dynamique was chosen to fabricate handsheets in order to provide multi-machine direction oriented sheets. Preliminary experiments were conducted with the unbleached high Kappa southern pine (HKSP) to determine the correct Jet-to-Wire ratio (JWR) to produce handsheets with a two-to-one, MD-to-CD tensile ratio.

Toward this end, the Formette jet velocity was fixed at 316 m/min, while the wire velocity was varied to obtain a JWR of 0.3 to 0.4. To simplify the pressing procedures, sheets were drained at a constant wire speed of 1050 m/min.

HKSP refined to three levels of freeness was formed at various JWRs, drained at constant speed, and conventionally pressed to 52% solids. Samples of these sheets were then tested to determine their darcian permeability as reported in terms of hydrodynamic specific surface. Figure 2 shows that specific surface may be reduced by reduced refining, while it was relatively insensitive to JWR. Samples were also cylinder dried, conditioned, and tested for MD and CD tensile strength. The MD/CD tensile ratio of these specimens is plotted as a function of JWR in Figure 3. As commercial liner typically has an MD/CD tensile ratio of about 2, subsequent experiments were conducted with sheets formed at a constant JWR of 0.4 corresponding to a wire speed of 800 m/min.

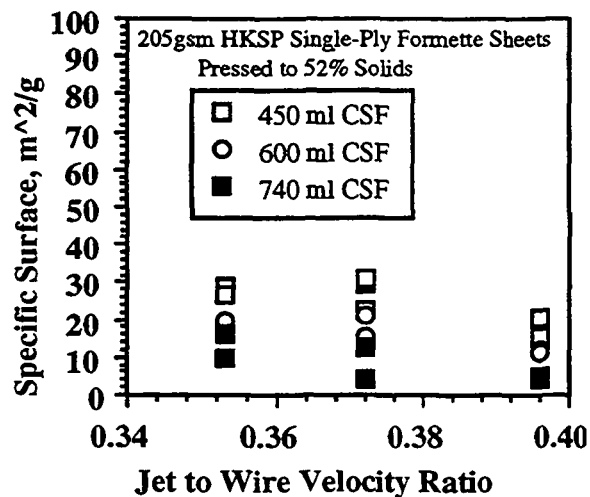


Figure 2. Hydrodynamic specific surface as a function of Jet-to-Wire velocity ratio for sheets pressed to 52% solids.

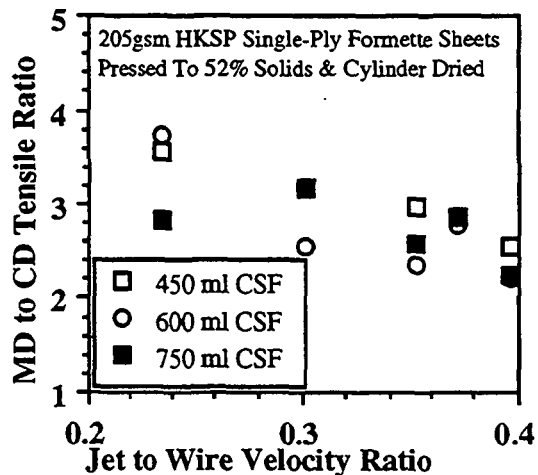


Figure 3. MD-to-CD tensile ratio as a function of Jet-to-Wire velocity ratio.

### Measurement of Fiber Dimensions

Samples of sheets prepared for impulse drying and double-felted pressing were coded and sent to John D. Hankey & Associates of Appleton, Wisconsin, for fiber species identification, fiber length, fiber width, cell wall thickness, and coarseness measurements.

Table 2 shows the results of the species identification for the furnish components used in the present research.

Table 2.  
Fiber Identification For Various Pulp Samples.

Pulp Type	USWK %	UHWK %	Softwood Species	Hardwood Species
S.Pine High Kappa	98	2	Southern yellow pine (Hard Cook)	Mixed, incl. Poplar
S.Pine Low Kappa	100(-)	trace	Southern yellow pine (Soft, Medium, & Hard Cook)	Mixed, incl. Gum
D.Fir High Kappa	99	1	40-50% Douglas Fir 40-50% Ponderosa or Lodgepole pine 5-10% Balsam Fir, 1% Western Hemlock 1% Engelman Spruce, 1% Western Pine 1% Western Red Cedar (Hard Cook)	Alder
D.Fir Low Kappa	99	1	70-80% Douglas Fir 5-10% Ponderosa or Lodgepole pine 5-10% Balsam Fir, 5% Western Red Cedar 5% Engelman Spruce, 1% Western White Pine, 1% Western Larch (Hard Cook)	Mixed, incl. Alder and Maple
OCC	76	24	80-90% Southern Yellow Pine 5-10% Douglas Fir, 1% Balsam Fir, 1% White and/or Red Pine, 1% Hemlock (53% Hard Cook, 18% Medium Soft Cook)	Mixed, incl. 20-30% Gum, 20-30% Oak, 10-20% Populus Sp., 10-20% Yellow Poplar, 5% Maple, 5% Elm, 5% Basswood, 5% Cherry, 5% Sycamore

Each of these furnishes was refined to various freeness levels and formed into 205 g/m<sup>2</sup> sheets. Table 3a and 3b summarize the average fiber dimensions.

Table 3a.  
Fiber Dimensions for Group I Sheets.  
(Single Furnish/ Single-Ply 205 g/m<sup>2</sup> Sheets Made on the Formette Dynamique)

Pulp Type	Kappa No.	Freeness ml CSF	Length mm			Width $\mu\text{m}$	Perimeter $\mu\text{m}$	Cell Wall Thickness $\mu\text{m}$	Coarseness mg/100 m
			Arith	LW	WW				
S.Pine	109.2 (High)	450	1.66	2.29	2.90	38.4	88.4	2.9	34.6
		600	1.77	2.47	3.11	40.7	93.0	2.9	35.6
		750	2.48	3.19	3.74	40.3	92.6	3.0	34.0
S.Pine	63.4 (Low)	450	1.88	2.64	3.31	38.3	88.6	3.0	30.4
		600	1.86	2.54	3.17	39.7	91.0	2.9	29.6
		710	2.60	3.29	3.78	41.5	92.2	2.3	30.8
D.Fir	89.6 (High)	450	1.20	1.59	2.00	35.8	80.4	2.2	23.2
		600	1.28	1.75	2.19	37.5	83.4	2.1	24.0
		720	2.02	2.69	3.20	38.3	85.8	2.3	23.8
D.Fir	74.2 (Low)	450	1.44	2.05	2.59	37.0	84.0	2.5	25.6
		600	1.75	2.38	2.89	39.1	87.8	2.4	25.2
		710	2.15	2.80	3.32	39.3	87.4	2.2	25.6
OCC	114.6 (High)	450	1.33	1.88	2.57	27.8	66.0	2.6	25.8
		600	1.54	2.20	2.93	29.2	68.8	2.6	24.8

Table 3b.  
Fiber Dimensions for Group III Sheets.  
(Two Furnish/Two-Ply 205 g/m<sup>2</sup> Sheets Made on the Formette Dynamique)

Wt. % HKSP 750 ml CSF in Bot.Ply	Wt. % OCC 600 ml CSF in Bot. Ply	Freeness of HKSP Heated Ply ml CSF	Length mm			Width $\mu\text{m}$	Perimeter $\mu\text{m}$	Cell Wall Thickness $\mu\text{m}$	Coarseness mg/100 m
			Arith	LW	WW				
40	40	450	1.81	2.56	3.28	34.9	81.0	2.8	31.4
40	40	600	1.63	2.51	3.38	32.9	77.8	3.0	32.0
40	40	750	1.95	2.78	3.46	31.9	76.2	3.1	31.8
0	80	450	1.51	2.24	2.99	30.0	71.6	2.9	27.0
0	80	750	1.58	2.47	3.34	32.1	75.8	2.9	26.2

### Hydrodynamic Specific Surface Measurements

Transverse permeability measurements were made using equipment and techniques previously reported (10). A schematic of the permeability apparatus is given in Figure 4. Not shown is the modified Carver press which generates the compressive loads required to measure permeability as a function of porosity in a saturated sheet.

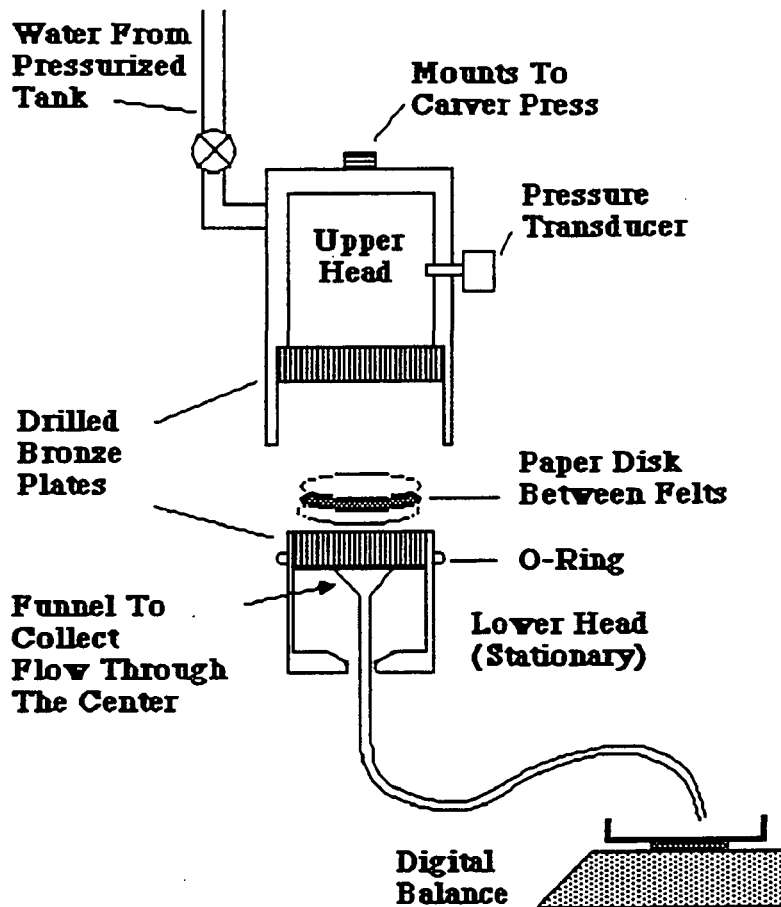


Figure 4. Schematic of the Transverse Permeability Measurement Apparatus.

In making transverse permeability measurements, a saturated paper disk was compressed between two wet felts. The felts were in contact with finely drilled bronze plates that transmit mechanical pressure while allowing water to flow through. To eliminate problems with leakage around the edge of the paper, only the flow through the central region (comprising 23% of the area of the paper disk) was collected and measured. This fluid entered a funnel which led the fluid through plastic tubing to a digital balance in order to measure the accumulated flow as a function of time. Sheet thickness was obtained using a Kaman eddy-current transducer.

In transverse permeability measurements, water passes through the central region of the paper and felts with a known pressure drop. The permeability is given by:

$$K_z = \frac{L}{\frac{A_{\text{flow}} \Delta P}{Q \mu} - R_f}$$

where  $A_{flow}$  is the cross-sectional area of the flow collection region (23% of the sheet area), and  $R_f$  is the inherent resistance of the felts and flow system.  $R_f$  was usually of little importance because the paper resistance was so much greater than the resistance of the felts or other components of the flow system. The other variables,  $L$ ,  $Q$ ,  $\Delta P$ , and  $\mu$ , are defined as sheet thickness, volumetric flow rate, pressure drops, and water viscosity, respectively.

Procedures described in Reference 10 were then used to determine the hydrodynamic specific surface.

### Double-Felted Pressing and Impulse Drying Simulations

Figure 5 shows a schematic of the electrohydraulic press used to simulate double-felted pressing and impulse drying. The apparatus was designed to simulate the transient mechanical and thermal conditions experienced during these processes. A newly installed programmable signal generator allowed the electrohydraulic press to simulate a pressure history that the sheet would experience in a commercial impulse dryer configured on a long-nip shoe press. For impulse drying simulations, thermal conditions were simulated using a ceramic-coated platen heated to the operating temperature of the process. As the dominant direction of flow is out-of-plane, the electrohydraulic press was expected to provide an excellent simulation of the processes under study.

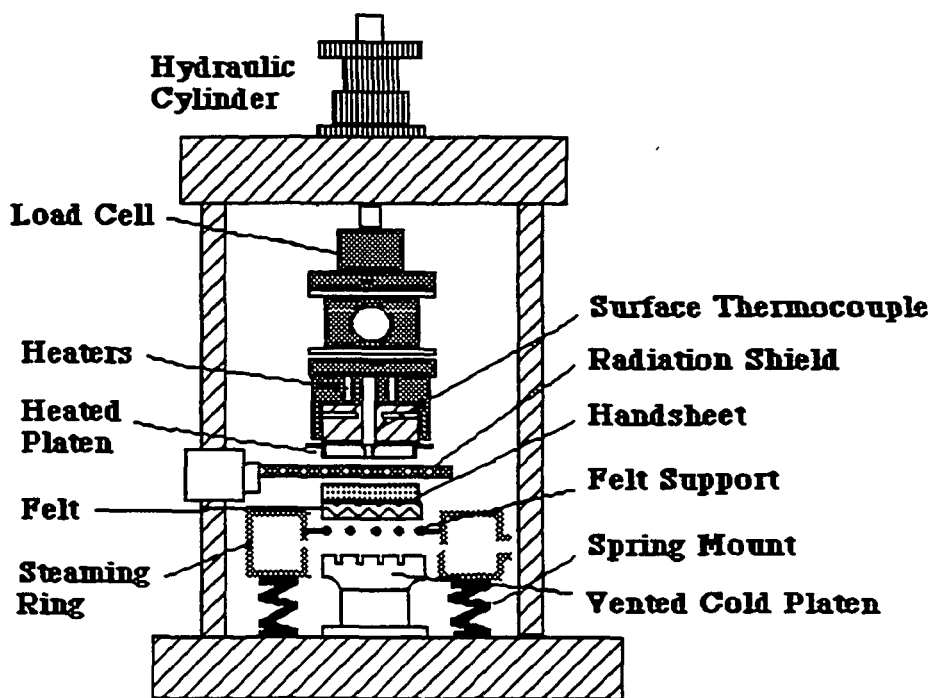


Figure 5. Schematic of the Electrohydraulic Press.

In impulse drying experiments, wet sheets of paper on felts were placed onto a wire felt support attached to a steaming ring. A radiation shield was automatically positioned between the heated platen and the sheet to reduce dry-out of the top surface of the sheet. Steam exiting from the ring flowed upward through the felt and the sheet. By controlling steam pressure and adjusting the steaming time, the initial temperature in the sheet was raised to 85°C. Once the sheet was heated, the hydraulic system was activated to give a pressure pulse of 40 millisecond duration simulating an 8500 pli load on a "0" pivot shoe press.

Double-felted pressing experiments were conducted in a similar manner, except that the platen was maintained at 100°C, and the wet sheet was sandwiched between two identical felts. For both double-felted pressing and impulse drying, the initial wet weight of the paper sheet was adjusted so that the ingoing dryness of the sheet after steam preheating was 52% solids +/- 2%. This required that water weight loss during steam pre-heating be calibrated as a function of initial platen temperature for each furnish. Ingoing felt moisture was kept at 16 percent.

## RESULTS

the folloing The results of the experiments will be presented in the following sections.

### Hydrodynamic Specific Surface

In this section, the out-of-plane permeability of single and two component single-ply sheets will be presented. Figures 6 and 7 show the hydrodynamic specific surface of single component single-ply sheets as a function of the Canadian standard freeness of the sheet. Figure 6 shows that the high Kappa southern pine tended to be more permeable at a given freeness than the low Kappa southern pine. In contrast, the low Kappa Douglas fir shown in Figure 7 was more permeable than the high Kappa Douglas fir. Contrasting the southern pine and Douglas fir at high freeness, it was observed that the southern pine tends to be more permeable.

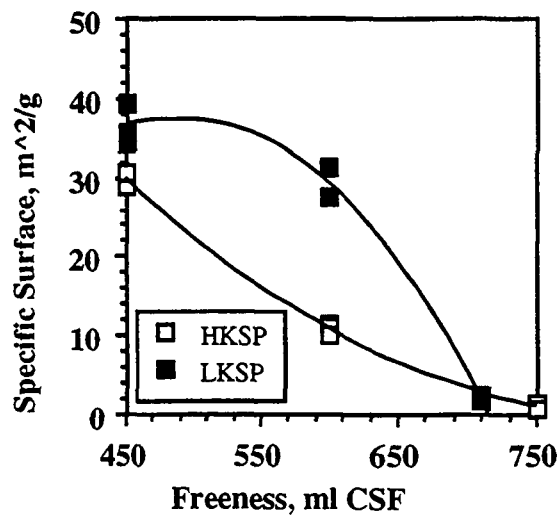


Figure 6. Specific surface vs. freeness for southern pine Kraft.

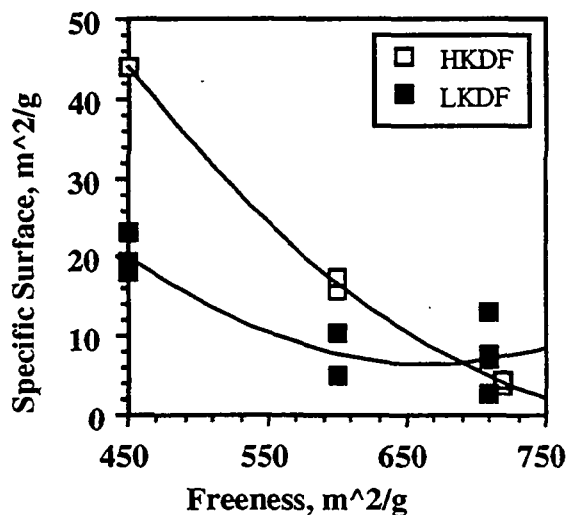


Figure 7. Specific surface vs. freeness for Douglas fir Kraft.

Similarly, hydrodynamic specific surface vs. freeness is shown for the OCC furnish in Figure 8. The specific surface of two component blends of high Kappa southern pine with OCC is shown as a function of the OCC content in Figure 9. It is of interest to note from Figure 9 that specific surface was not a linear function of OCC content. Hence, as much as 60% OCC by weight can be added to the blend without the hydrodynamic specific surface increasing beyond 5 m<sup>2</sup>/g.

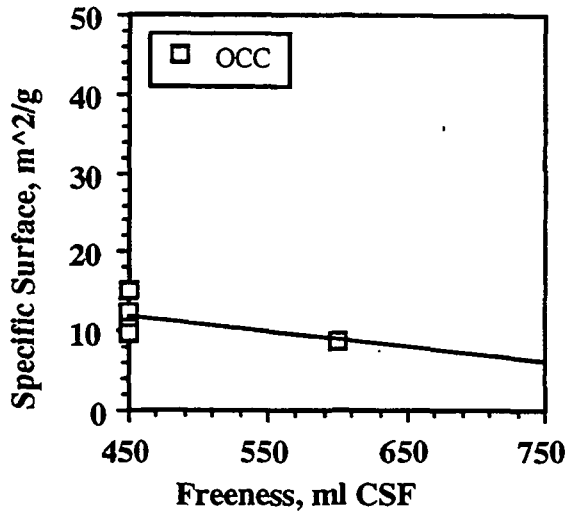


Figure 8. Specific surface vs. freeness for OCC.

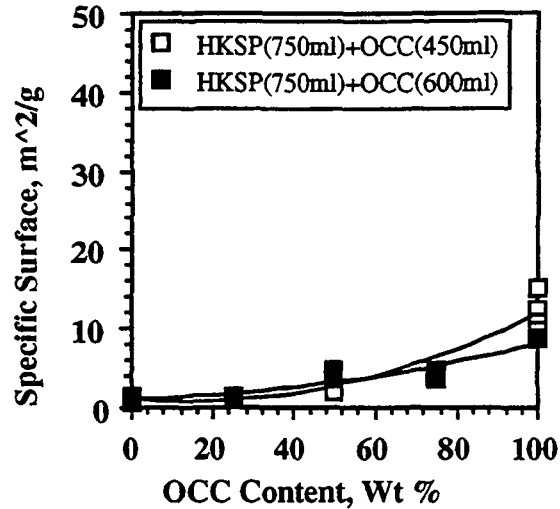


Figure 9. Specific surface vs. OCC content for single ply-blends of southern pine and OCC.

It was also observed that for the single-ply linerboard that was impulse dried, see Table 1, the hydrodynamic specific surface was a linear function of the weight weighted fiber length that made up the sheet. This relationship is shown in Figure 10. It should be recalled that weight weighted fiber length is primarily a function of the fines concentration. Hence, sheet permeability was primarily influenced by fines concentration.

### Critical Temperature

Previous research has shown that the critical impulse drying temperature, defined as the platen temperature above which sheet delamination occurs, decreases with increasing hydraulic specific surface. That work, with single-ply sheets made from a single furnish, also showed that the benefits of impulse drying as compared to single-felted extended nip pressing decreased as the critical temperature decreased.

As in the previous work, the critical temperatures in these experiments have been determined by visual inspection and interpretation of out-of-plane ultrasound (specific elastic modulus) data and STFI compression strength data. The procedure was to define the critical temperature as the lowest temperature that showed no signs of delamination. The specific elastic modulus and its coefficient of variation were typically the most sensitive indicators. Figures A1 through A30 in the Appendix show the coefficient of variation of the elastic modulus and its mean value plotted against initial platen surface temperature. In each of these figures, delamination occurs when the coefficient of variation suddenly rises or when the modulus suddenly drops with increased initial platen

temperature. In Figure 11, the critical temperature for the present experiments is plotted as a function of the hydrodynamic specific surface. For single-ply sheets, the hydrodynamic specific surface was the measured value for that sheet as per Figures 6 through 9. For two-ply sheets, the hydrodynamic specific surface was assumed to be that of the surface of the sheet in contact with the heated platen. Data from previous work on the Institute's pilot roll press are also shown for comparison in Figure 11.

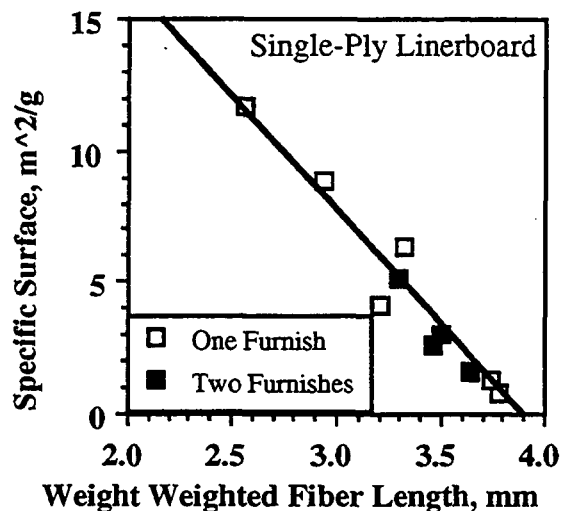


Figure 10. Hydrodynamic specific surface vs. weight weighted fiber length for single-ply linerboard pressed to 52% solids.

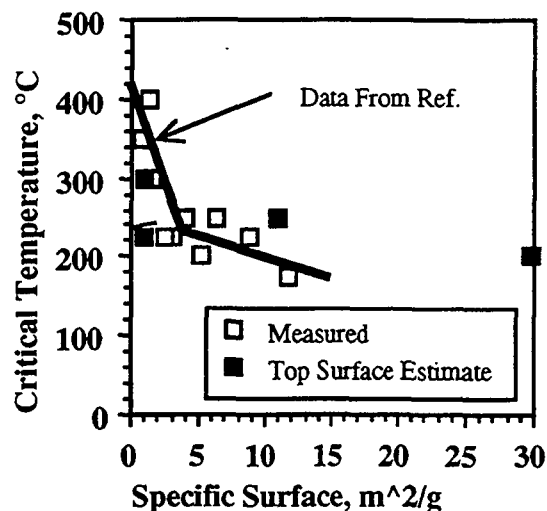


Figure 11. Critical impulse drying temperature vs. hydrodynamic specific surface for single- and double-ply linerboard.

The fact that the double-ply and single-ply data are consistent demonstrates that it is the hydrodynamic specific surface of the layer in contact with the heated platen (the top layer) that controls delamination.

The effect on critical temperature of increasing the concentration of OCC in a blend with HKSP is shown in Figure 12. It is observed that critical temperature decreases with increasing OCC content. The influence of the permeability of the layer in contact with the heated platen surface is again observed in Figure 13, where critical temperature increases when the extent of refining is reduced (i.e., higher freeness).

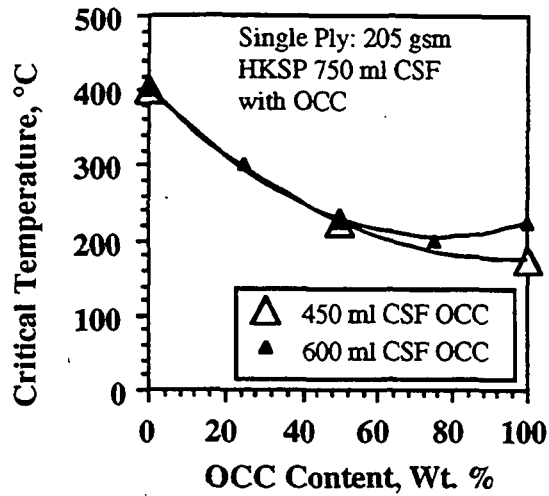


Figure 12. Critical impulse drying temperature vs. OCC content for single-ply sheets.

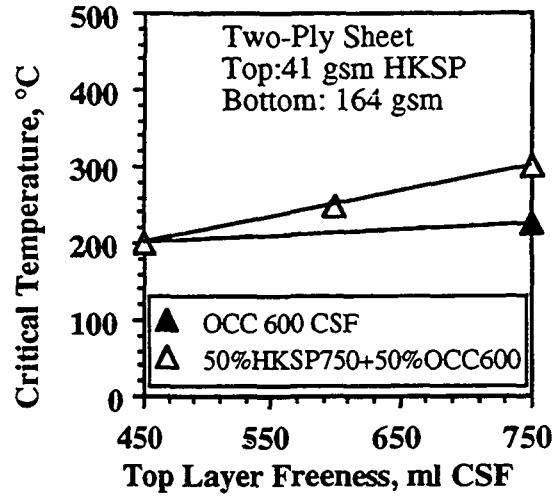


Figure 13. Critical impulse drying temperature vs. top layer freeness for double-ply sheets.

### Impulse Drying vs. Double-felted Pressing

In the next series of figures, impulse drying at the critical temperature is compared to double-felted pressing and to a control that was pressed to 52% solids and cylinder dried. Figures 14 and 15 show outgoing solids vs. OCC content for single-ply sheets made from high Kappa southern pine and old corrugated containers. It is observed that impulse drying has a press dryness advantage over double-felted pressing for OCC content below 60%.

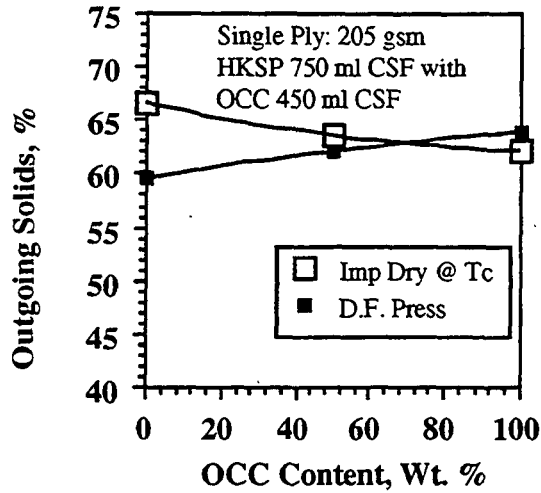


Figure 14. Outgoing solids vs. OCC content for impulse drying and double-felted pressing with blends of HKSP750 and OCC450.

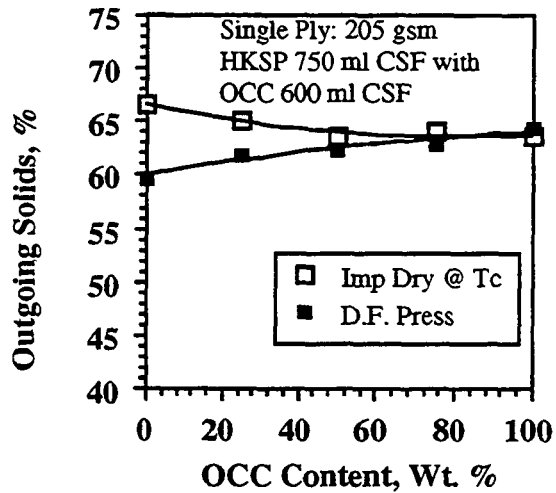


Figure 15. Outgoing solids vs. OCC content for impulse drying and double-felted pressing with blends of HKSP750 and OCC600.

Figures 16 and 17 show outgoing solids vs. top layer freeness for double-ply sheets where the two bottom layer blends are considered. When the bottom layer was made from a 50%:50% blend of HKSP750 and OCC600, impulse drying was superior to double-felted pressing independent of top layer freeness. For the case when the bottom layer was made from 100% OCC600, impulse drying was superior when the top layer freeness was more than 600 ml CSF.

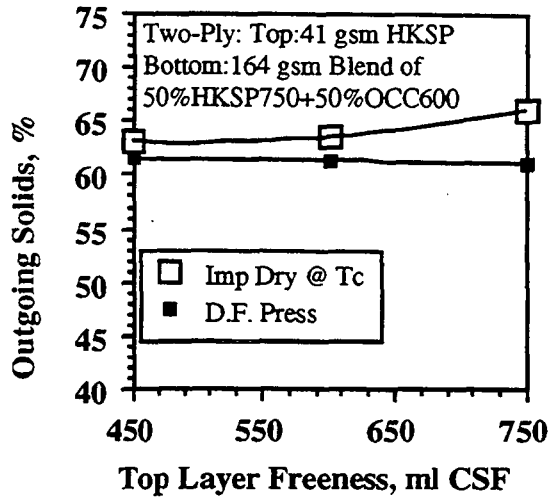


Figure 16. Outgoing solids vs. top layer freeness for impulse drying and double-felted pressing with bottom layer of 50%HKSP750 and 50% OCC600 with HKSP top layer.

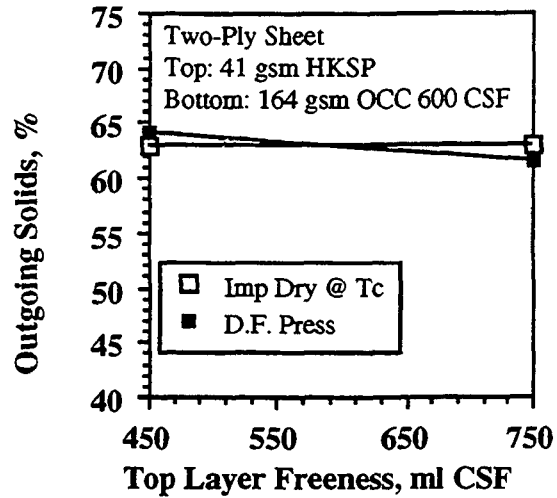


Figure 17. Outgoing solids vs. top layer for impulse drying and double-felted pressing with OCC600 bottom layer and HKSP top layer.

Many linerboard manufacturers use the cross direction STFI compression strength as the target strength parameter used to adjust their processes. Hence, the higher the CD STFI Index the better. Figures 18 and 19 show CD STFI Index vs. OCC content for single-ply sheets made from high Kappa southern pine and old corrugated containers. In Figures 14 and 15, it was observed that impulse drying dryness was superior to double-felted pressing dryness for OCC content below 60%. In Figures 18 and 19, impulse drying CD STFI Index was superior to that of double-felted pressing as long as OCC content was below 50%. Comparing the CD STFI Index obtained by impulse drying to that of the control shows that impulse drying has a benefit over conventional papermaking independent of OCC content.

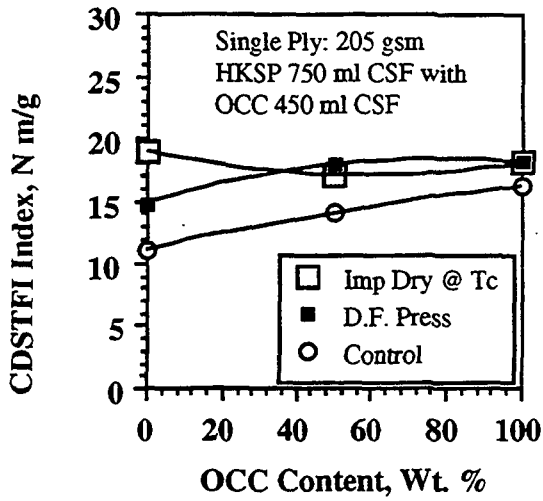


Figure 18. CD STFI Index vs. OCC content for impulse drying and double-felted pressing with blends of HKSP750 and OCC450.

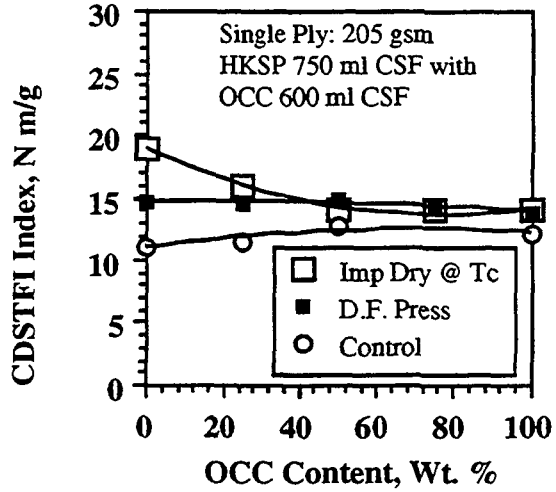


Figure 19. CD STFI Index vs. OCC content for impulse drying and double-felted pressing with blends of HKSP750 and OCC600.

Figures 20 and 21 show CD STFI Index vs. top layer freeness for double-ply sheets. When the bottom layer was made from a 50%:50% blend of HKSP750 and OCC600, impulse drying CD STFI Index was superior to that of double-felted pressing when top layer freeness was greater than 550 ml CSF. When the bottom layer was made from 100% OCC600, impulse drying CD STFI Index was equal or superior for the entire range of top layer freeness. Observe that impulse drying always resulted in superior strength as compared to the control.

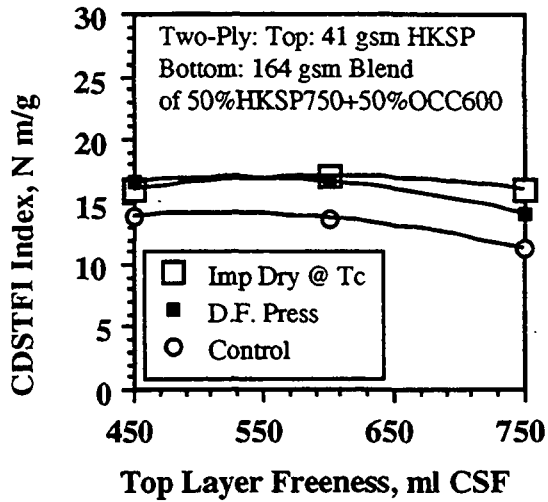


Figure 20. CD STFI Index vs. top layer freeness for impulse drying and double-felted pressing with bottom layer of 50%HKSP750 and 50%OCC600 with HKSP top layer.

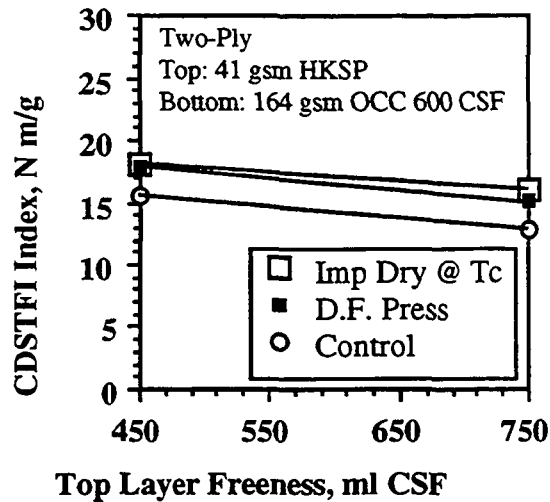


Figure 21. CD STFI Index vs. top layer for impulse drying and double-felted pressing with OCC600 bottom layer and HKSP top layer.

In designing the structure of linerboard sheets, manufacturers need to consider the physical appearance of the top layer of the sheet. In this regard, impulse drying consistently yields a smoother surface than alternate processes. Another important design parameter is the color of the top layer. Figures 22 and 23 give  $L^*$ ,  $a^*$ ,  $b^*$  color measurements from the top surface of impulse dried sheets. Notice color is generally independent of OCC content and independent of the freeness of the top surface. In a separate result, cracking angles of impulse dried sheets were found to be greater than  $90^\circ$ .

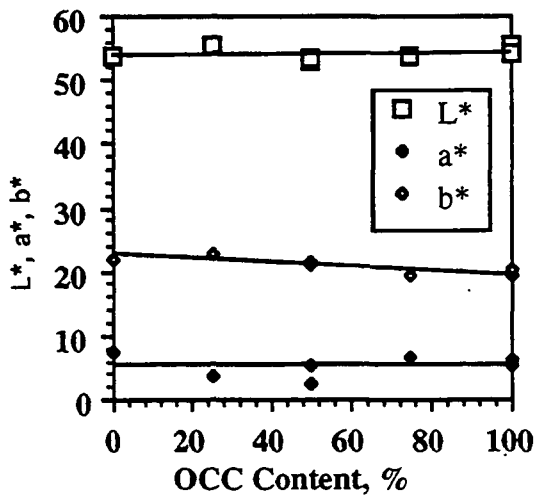


Figure 22.  $L^*$ ,  $a^*$ ,  $b^*$  vs. OCC content for single-ply impulse dried sheets.

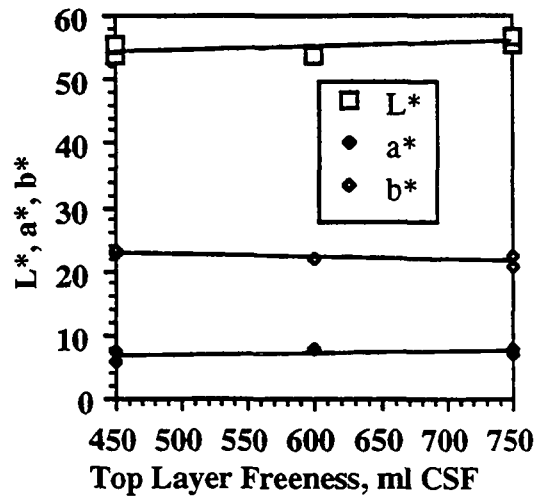


Figure 23.  $L^*$ ,  $a^*$ ,  $b^*$  vs. top layer freeness for double-ply impulse dried sheets.

MD STFI Index and density are also given for reference in Figures 24 through 31.

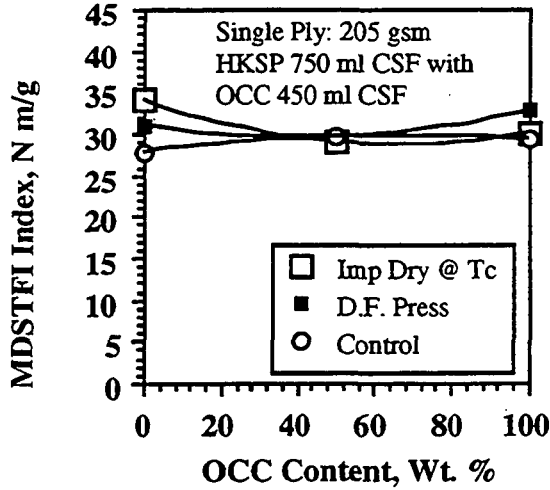


Figure 24. MD STFI Index vs. OCC content for impulse drying and double-felted pressing with blends of HKSP750 and OCC450.

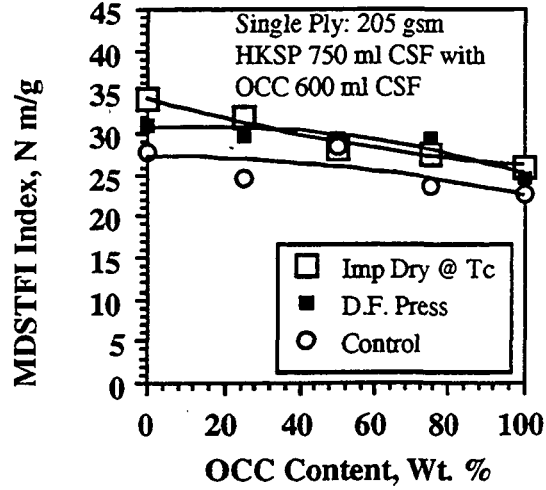


Figure 25. MD STFI Index vs. OCC content for impulse drying and double-felted pressing with blends of HKSP750 and OCC600.

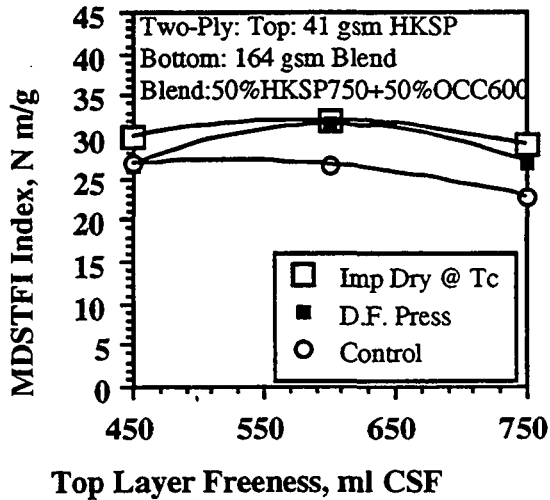


Figure 26. MD STFI Index vs. top layer freeness for impulse drying and double-felted pressing with bottom layer of 50%HKSP750 and 50% OCC600 with HKSP top layer.

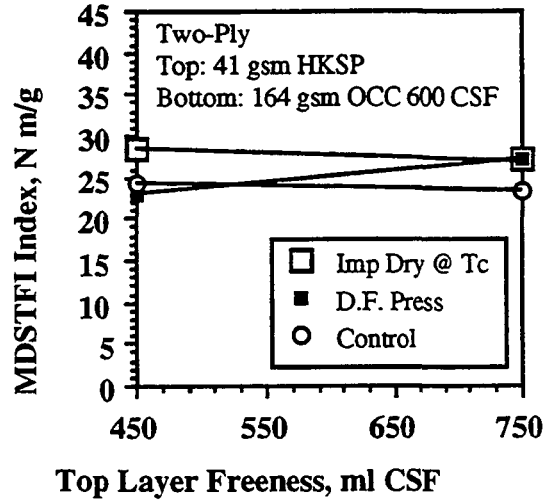


Figure 27. MD STFI Index vs. top layer freeness for impulse drying and double-felted pressing with OCC600 bottom layer HKSP top layer.

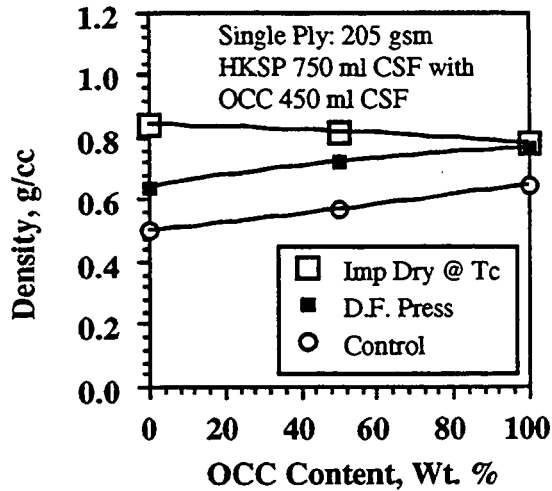


Figure 28. Density vs. OCC content for impulse drying and double-felted pressing with blends of HKSP750 and OCC450.

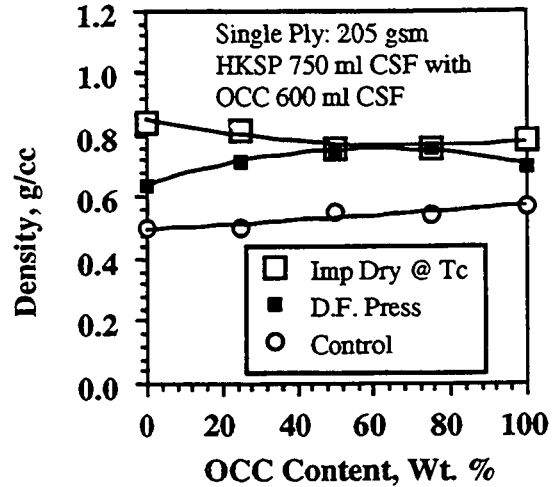


Figure 29. Density vs. OCC content for impulse drying and double-felted pressing with blends of HKSP750 and OCC600.

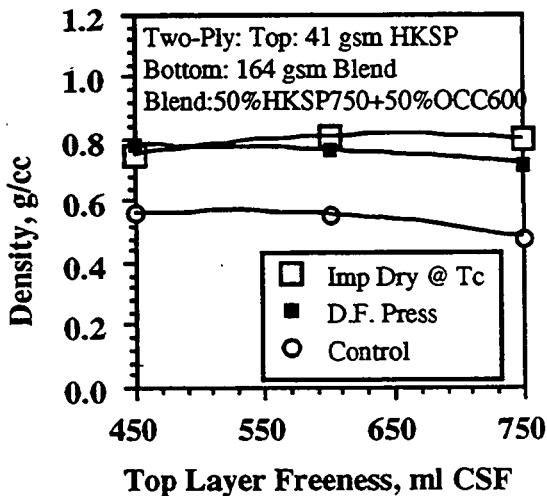


Figure 30. Density vs. top layer freeness for impulse drying and double-felted pressing with bottom layer of 50%HKSP750 and 50%OCC600 with HKSP top layer.

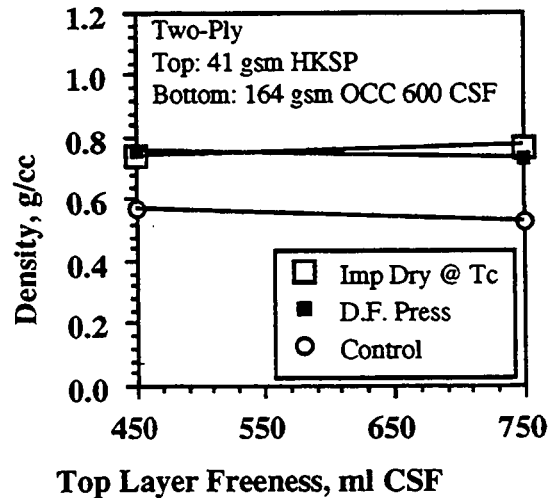


Figure 31. Density vs. top layer for impulse drying and double-felted pressing with OCC600 bottom layer and HKSP top layer.

## CONCLUSIONS

Preliminary experiments identified procedures for operating the Formette Dynamique to achieve the correct fiber orientation and to map out the influence of refining on fiber morphology and sheet permeability. The major result of these preliminary experiments was to show that Z-directional permeability is nearly independent of fiber orientation in the sheet while being strongly dependent on refining. In particular, the refining effect on permeability was found to be species dependent in that Douglas fir was less permeable to water transport than was southern pine at high freeness levels. This in turn, was traced to the higher fines concentration of the Douglas fir.

In the first experimental group, single-ply 42 lb liner made from five minimally refined furnishes was impulse dried to explore the influence of fiber species and lignin content on impulse drying. In these experiments, high and low Kappa southern pine and Douglas fir were evaluated, as was a OCC furnish. The major conclusions of this part of the work were that Kappa number had little effect on impulse drying performance, while southern pine was found to have an advantage over Douglas fir. As a result of southern pine having lower fines concentration at high freeness, it could be impulse dried at higher temperatures resulting in higher outgoing dryness and enhanced physical properties.

The second group of experiments was designed to answer the question of how much recycled fiber could be blended with virgin Kraft and still be successfully impulse dried. Here, the criterion for success was that the strength and dryness imparted by impulse drying be superior to that which could be achieved by conventional double-felted pressing at the same impulse as used during impulse drying. In these experiments, single-ply sheets were formed from blends of OCC refined to two different freenesses with a lightly refined virgin southern pine. Here, southern pine was chosen based on the results of the first group of experiments. The general conclusion of the second group of experiments was that the strength advantage of impulse drying was observed at recycle concentrations of 50 percent or less, while a dryness advantage was observed for blends having recycle concentrations of 75 percent or less.

In the third group of experiments, two-ply sheets of various constructions were impulse dried to determine how the composition of the top and bottom layer influences optimum impulse drying operating conditions and resulting dryness and physical properties. The major conclusion was that the composition of that part of the sheet in contact with the heated surface controls the critical impulse drying temperature. When the bottom sheet was composed of 50 percent virgin Kraft and 50 percent recycled fiber, superior impulse drying dryness and physical property development were observed for top sheet compositions having freenesses of 450 ml CSF or more. Sheets constructed with a bottom sheet of recycled fiber and a top sheet of virgin Kraft showed enhanced dryness and strength as long as the heated surface of the sheet had a freeness of 600 ml CSF or more.

## RECOMMENDATIONS

The first year's work has demonstrated that multi-ply linerboard having significant concentrations of recycle fiber can be successfully impulse dried.

In the second year, the laboratory-scale database will be extended to include three-ply sheets and furnishes composed of blends of Douglas fir and recycled fiber. In addition, the results of the first year will be confirmed in batch pilot-scale experiments.

## REFERENCES

1. Orloff, D.I., "High-Intensity Drying Processes - Impulse Drying Report Four," U.S. Department Of Energy Report No. DOE/CE/40738-T4, (May 1989).
2. Orloff, D.I., "Impulse Drying of Paper - Fundamentals of Delamination and Its Control," Presented at the Annual Meeting of the American Society of Chemical Engineers, (November 1989).
3. Orloff, D.I., "High-Intensity Drying Processes - Impulse Drying Report Five," U.S. Department Of Energy Report No. DOE/CE/40738-T5, (September 1990).
4. Orloff, D.I., "Impulse Drying of Linerboard: Control of Delamination," Journal of Pulp and Paper Science, 18(1), J23-J32 (January 1992). Also presented at the 77th Annual Meeting of the Technical Section of the Canadian Pulp and Paper Association, (January 1991).
5. Orloff, D.I., "Impulse Drying: Heterogeneous Press Surfaces Offer New Product Opportunities," Tappi Journal 75(5): 172-176 (May 1992). Also presented at the TAPPI Non-wovens Conference (May 1991).
6. Orloff, D.I., "Impulse Drying: Controlling Delamination in Heavy Weight Grades," IPST Executives' Conference, Atlanta, GA, (May 1991).
7. Orloff, D.I., "High-Intensity Drying Processes - Impulse Drying Report Six," U.S. Department Of Energy Report No. DOE/CE/40738-T6, (July 1991).
8. Orloff, D.I., et al., Method and Apparatus for Drying Web, U.S. Patent Number 5101574, Issued April 7, 1992.
9. Orloff, D.I., "Impulse Drying of Paper: A Review of Recent Research," 14th Industrial Energy Technology Conference, Houston, TX, (April 1992).
10. Orloff, D.I., and Lindsay, J.D., "The Influence of Yield, Refining and Ingoing Solids on the Impulse Drying Performance of a Ceramic Coated Press Roll," TAPPI Papermakers Conference, Nashville, TN, (April 1992).
11. Orloff, D.I., and Lindsay, J.D., "Advances in Wet Pressing," IPST Executives' Conference, Atlanta, GA, (May 1992).
12. Orloff, D.I., and Sobczynski, S.F., "Impulse Drying Pilot Press Demonstration: Ceramic Surfaces Inhibit Delamination," SPCI'92 ATICELCA Conference "The 4th New Available Techniques," Bologna, Italy, (May 1992).
13. Lenling, W.J., Smith, M.F., and Orloff, D.I., "Thermal Coating Development for Impulse Drying," International Thermal Spray Conference, Orlando, FL, (June 1992). (Given Best Paper Of Conference Award).
14. Orloff, D.I., Jones, G.L., and Phelan, P.M., "Effects of Heating Mode on Roll Durability and Efficiency of Impulse Drying," 28th National Heat Transfer Conference-Session on Fundamentals of Heat Transfer in Porous Media, San Diego, CA, (August 1992).

15. Orloff, D.I., "A Comparison of Impulse Drying to Double Felted Pressing on Pilot-Scale Shoe Presses and Roll Presses," U.S. Department Of Energy Report No. DOE/CE/40738-T7, (August 1992).

#### ACKNOWLEDGMENTS

The author would like to thank members of the Impulse Drying Research Team for their assistance in conducting the experiments described in this report. The author would like to specifically thank Dr. Isaac Rudman for his assistance.

The author and the Impulse Drying Research Team also wish to thank the members of the CKPG Advisory Group for their support, advice, and assistance throughout the course of these experiments.

APPENDIX

Specific Elastic Modulus and its Coefficient of Variation

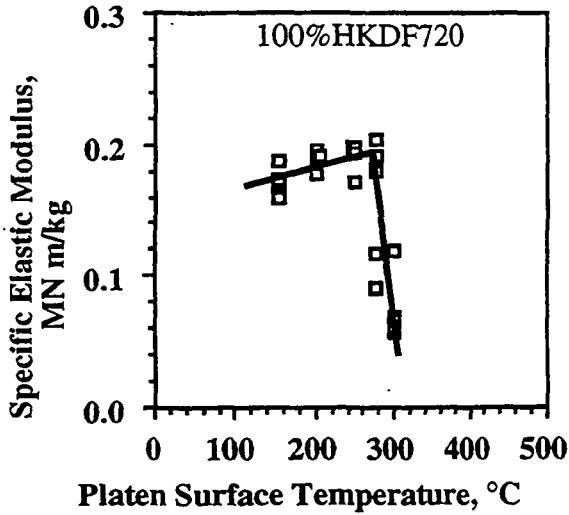


Figure A1. Specific elastic modulus vs. initial platen surface temperature for HKDF720.

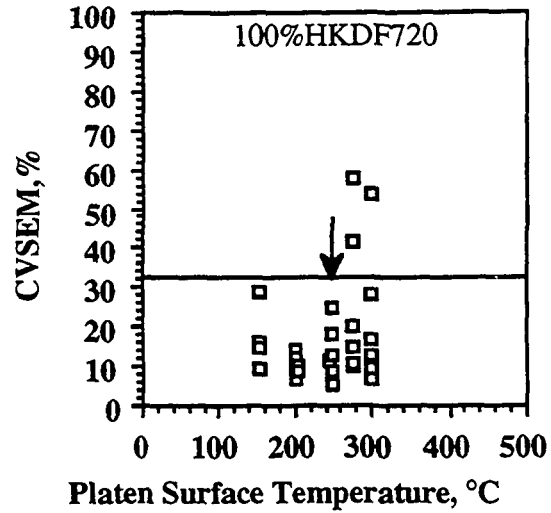


Figure A2. Coefficient of variation of the specific elastic modulus vs. initial platen surface temperature for HKDF720.

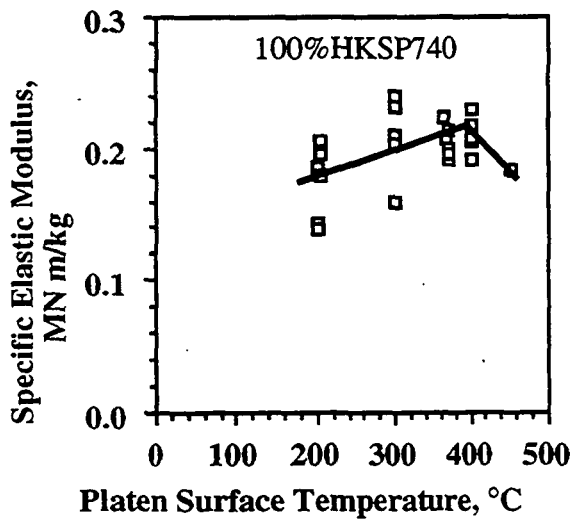


Figure A3. Specific elastic modulus vs. initial platen surface temperature for HKSP740.

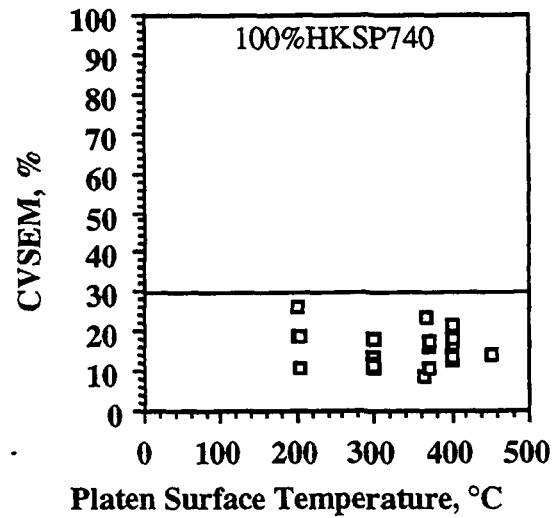


Figure A4. Coefficient of variation of the specific elastic modulus vs. initial platen surface temperature for HKSP740.

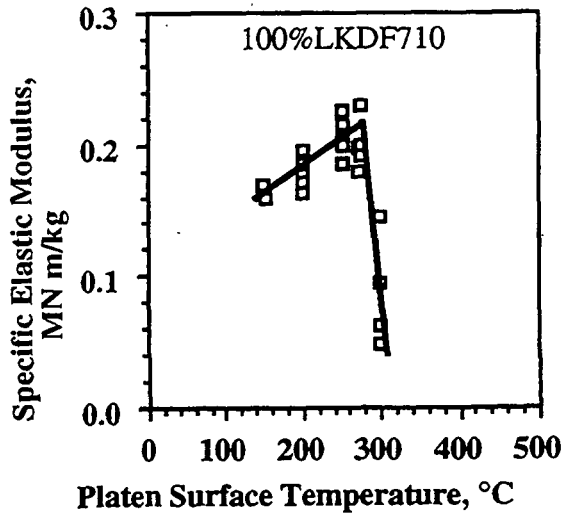


Figure A5. Specific elastic modulus vs. initial platen surface temperature for LKDF710.

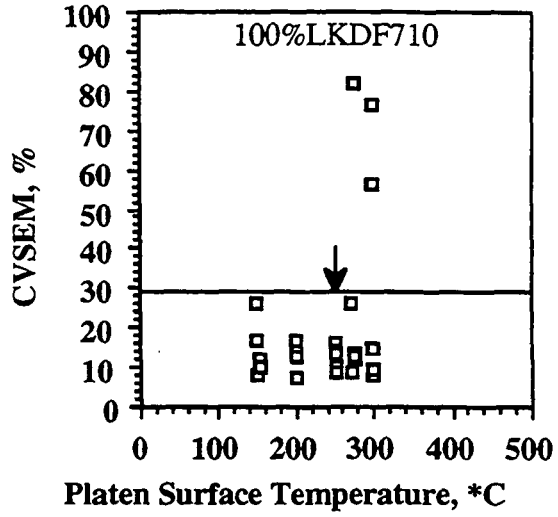


Figure A6. Coefficient of variation of the specific elastic modulus vs. initial platen surface temperature for LKDF710.

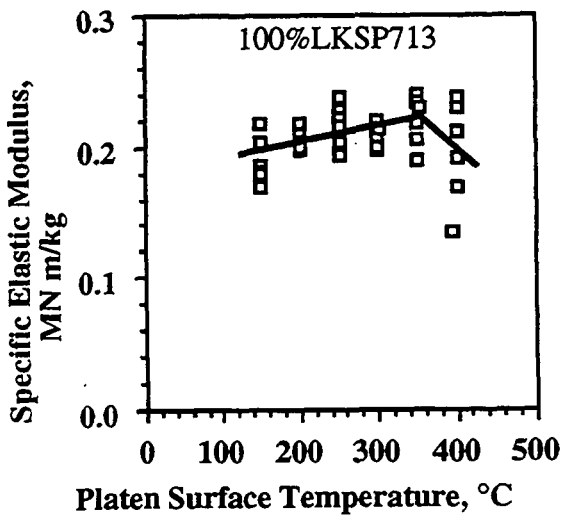


Figure A7. Specific elastic modulus vs. initial platen surface temperature for LKSP713.

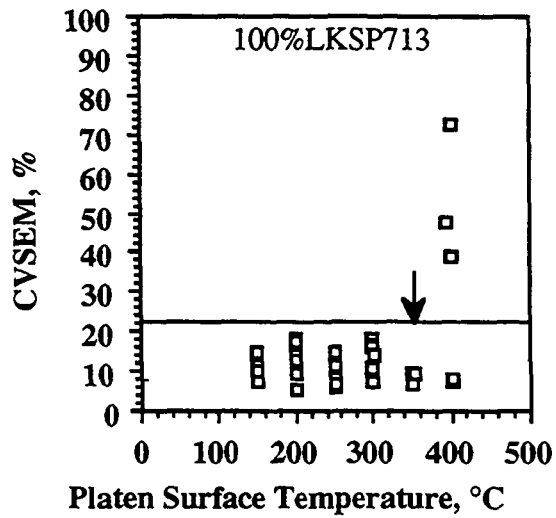


Figure A8. Coefficient of variation of the specific elastic modulus vs. initial platen surface temperature for LKSP713.

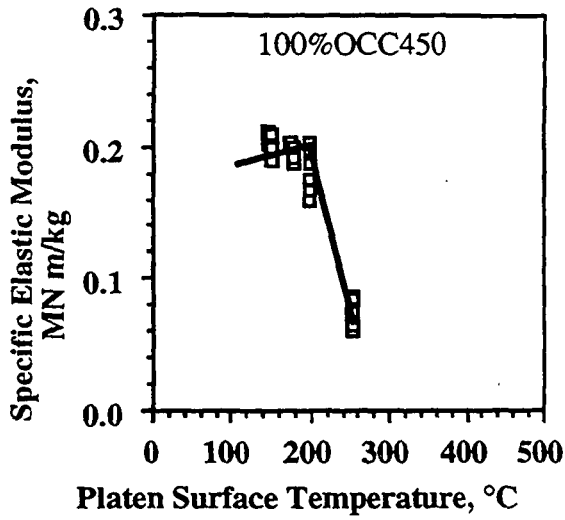


Figure A9. Specific elastic modulus vs. initial platen surface temperature for OCC450.

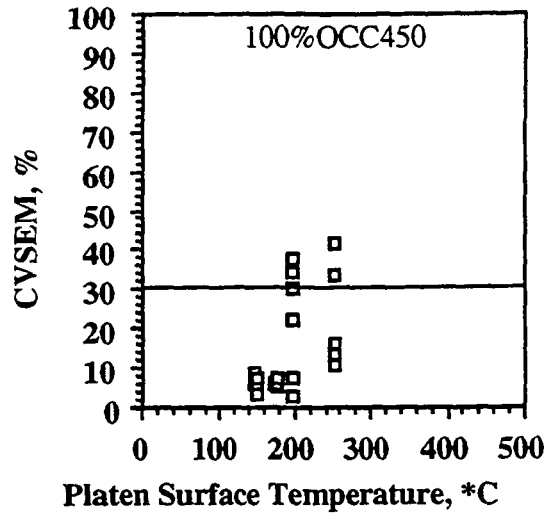


Figure A10. Coefficient of variation of the specific elastic modulus vs. initial platen surface temperature for OCC450.

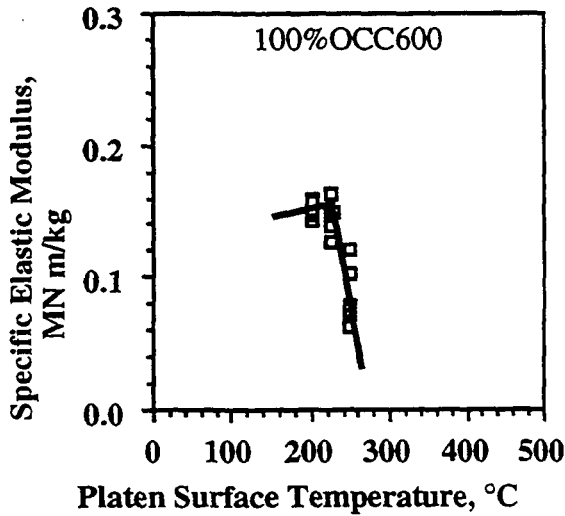


Figure A11. Specific elastic modulus vs. initial platen surface temperature for OCC600.

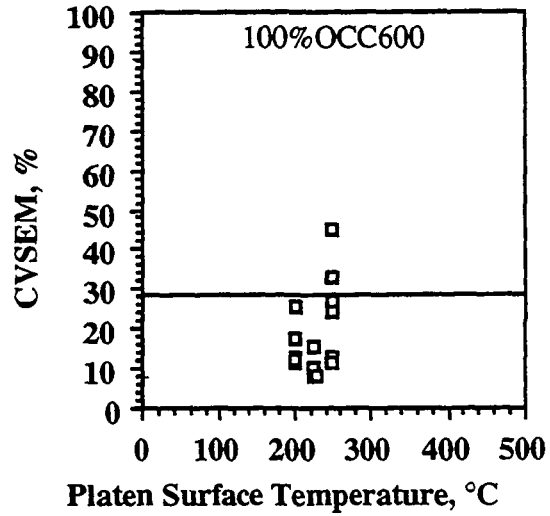


Figure A12. Coefficient of variation of the specific elastic modulus vs. initial platen surface temperature for OCC600.

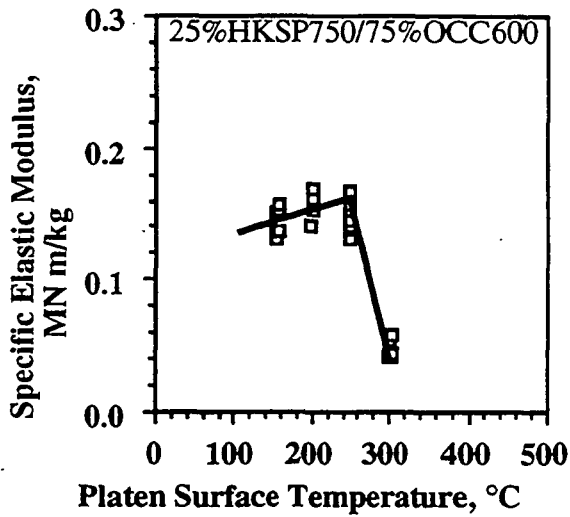


Figure A13. Specific elastic modulus vs. initial platen surface temperature for 25%HKSP750/75%OCC600.

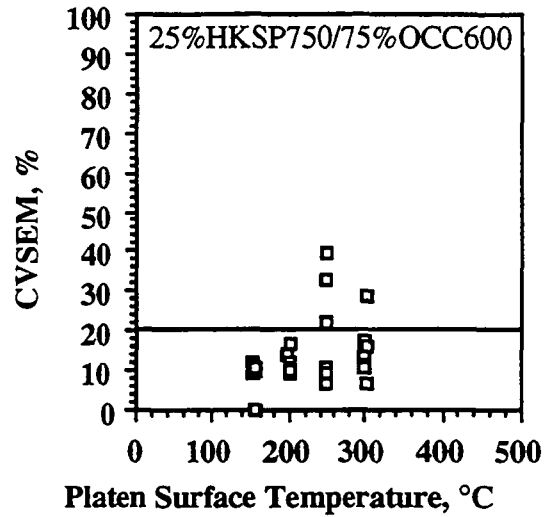


Figure A14. Coefficient of variation of the specific elastic modulus vs. initial platen surface temperature for 25%HKSP750/75%OCC600.

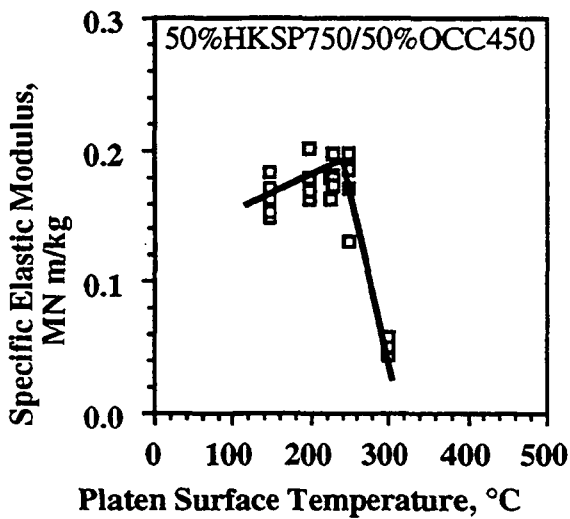


Figure A15. Specific elastic modulus vs. initial platen surface temperature for 50%HKSP750/50%OCC450.

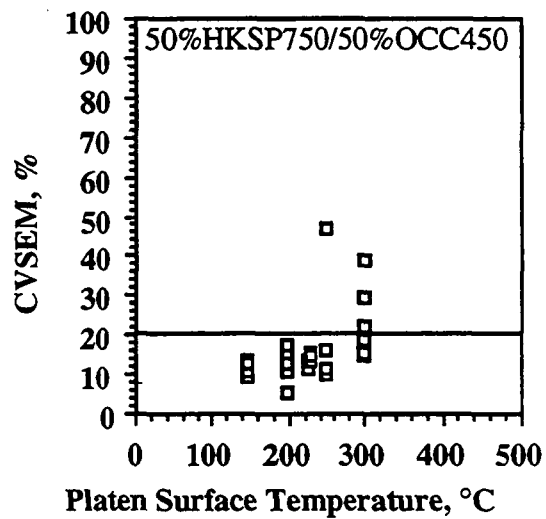


Figure A16. Coefficient of variation of the specific elastic modulus vs. initial platen surface temperature for 50%HKSP750/50%OCC450.

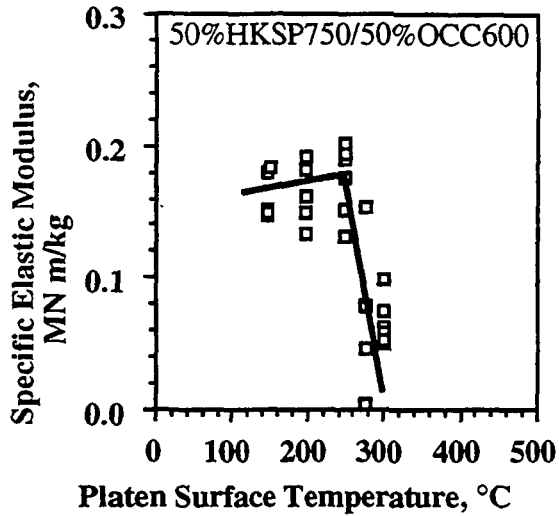


Figure A17. Specific elastic modulus vs. initial platen surface temperature for 50%HKSP750/50%OCC600.

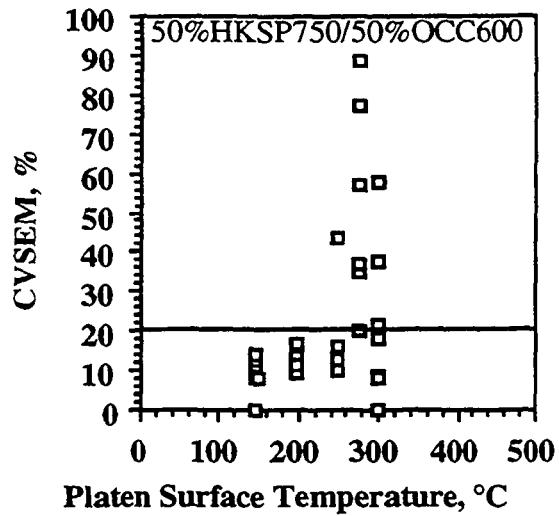


Figure A18. Coefficient of variation of the specific elastic modulus vs. initial platen surface temperature for 50%HKSP750/50%OCC600.

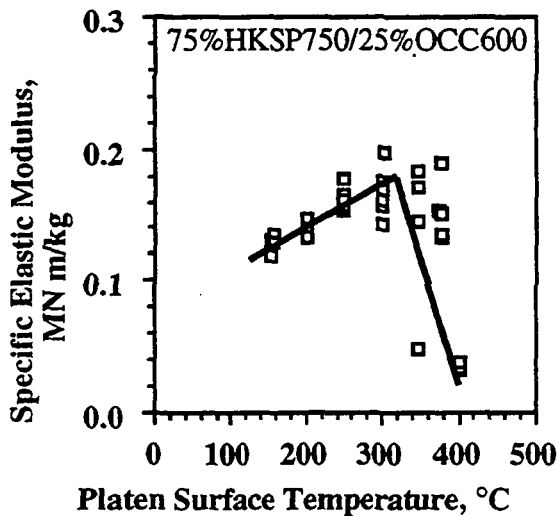


Figure A19. Specific elastic modulus vs. initial platen surface temperature for 75%HKSP750/25%OCC600.

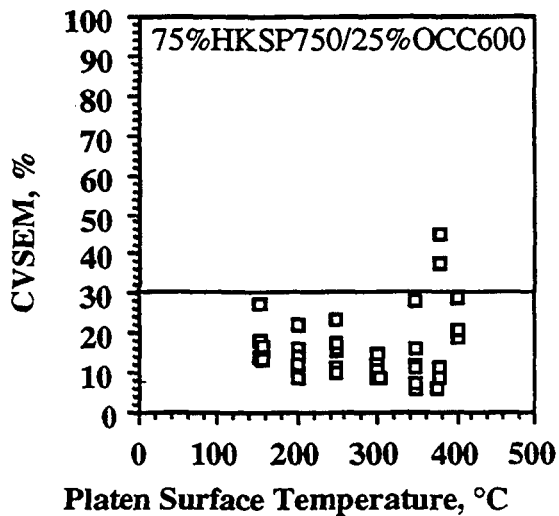


Figure A20. Coefficient of variation of the specific elastic modulus vs. initial platen surface temperature for 75%HKSP750/25%OCC600.

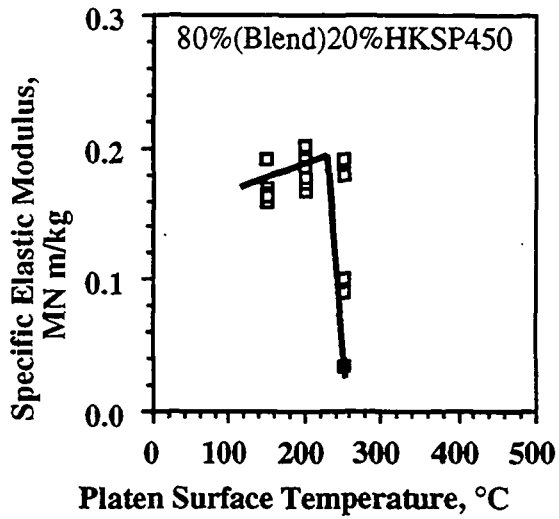


Figure A21. Specific elastic modulus vs. initial platen surface temperature for 80%(Blend)20%HKSP450.

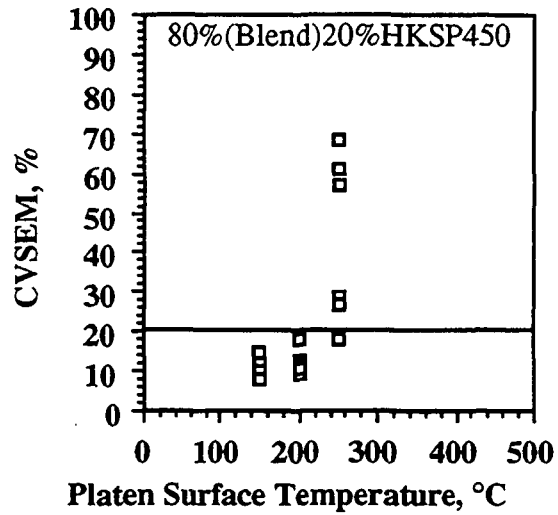


Figure A22. Coefficient of variation of the specific elastic modulus vs. initial platen surface temperature for 80%(Blend)20%HKSP450.

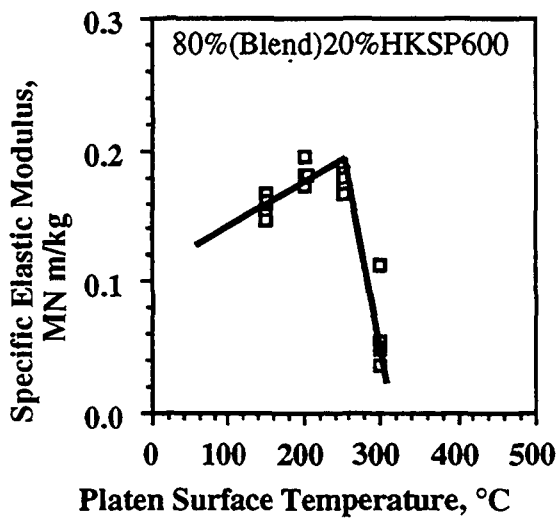


Figure A23. Specific elastic modulus vs. initial platen surface temperature for 80%(Blend)20%HKSP600.

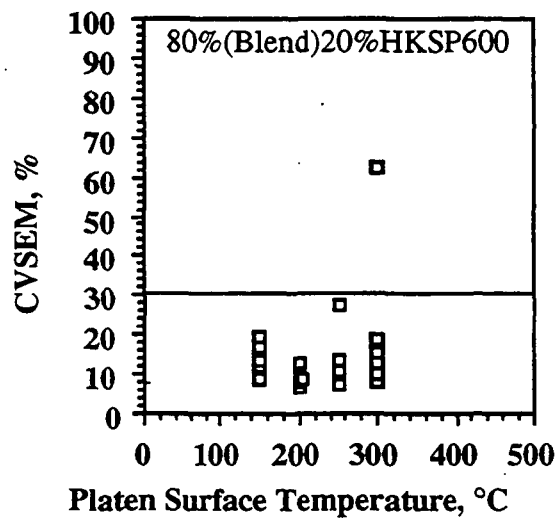


Figure A24. Coefficient of variation of the specific elastic modulus vs. initial platen surface temperature for 80%(Blend)20%HKSP600.

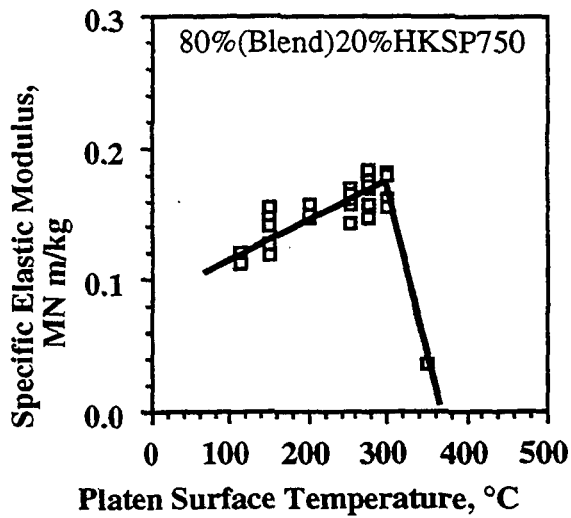


Figure A25. Specific elastic modulus vs. initial platen surface temperature for 80%(Blend)20%HKSP750.

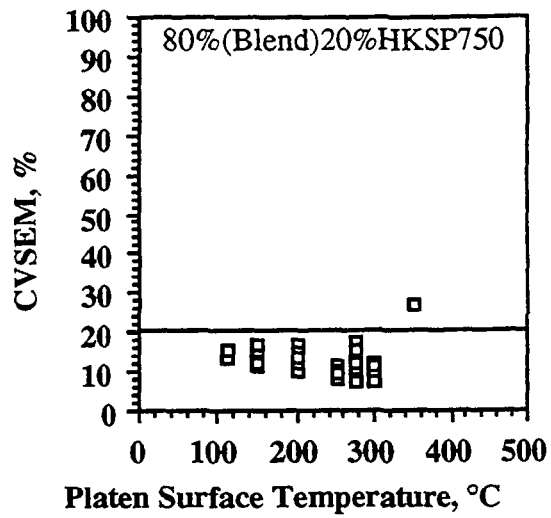


Figure A26. Coefficient of variation of the specific elastic modulus vs. initial platen surface temperature for 80%(Blend)20%HKSP750.

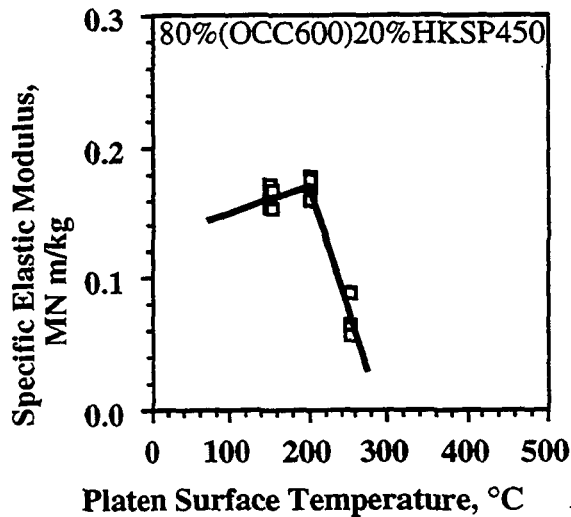


Figure A27. Specific elastic modulus vs. initial platen surface temperature for 80%(OCC600)20%HKSP450.

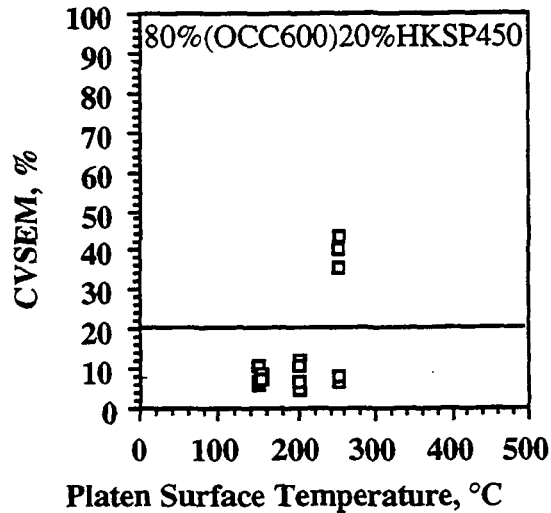


Figure A28. Coefficient of variation of the specific elastic modulus vs. initial platen surface temperature for 80%(OCC600)20%HKSP450.

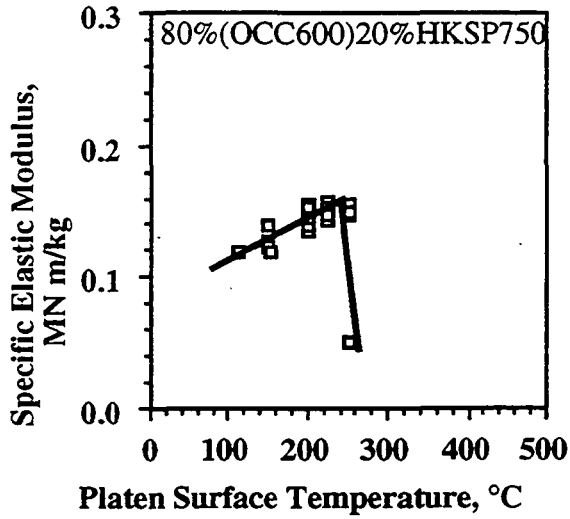


Figure A29. Specific elastic modulus vs. initial platen surface temperature for 80%(OCC600)20%HKSP750.

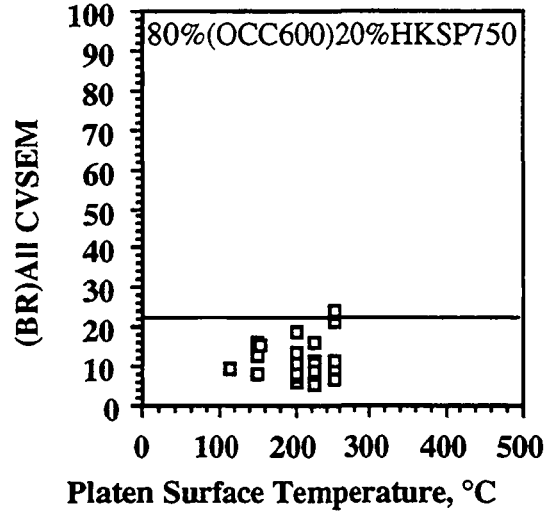


Figure A30. Coefficient of variation of the specific elastic modulus vs. initial platen surface temperature for 80%(OCC600)20%HKSP750.

**Outgoing Solids vs. Initial Platen Surface**

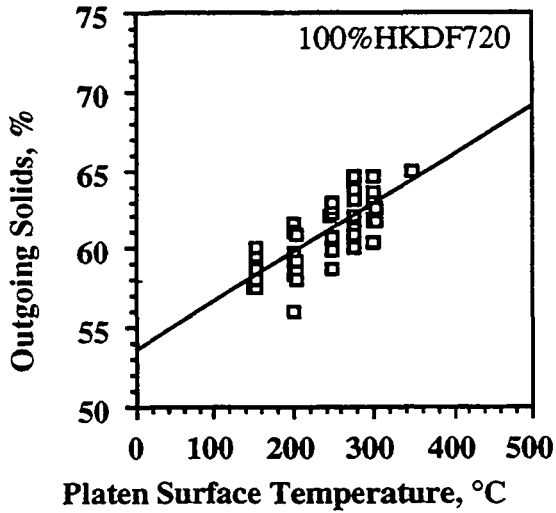


Figure A31. Outgoing solids vs. initial platen surface temperature for impulse drying of 100%HKDF720.

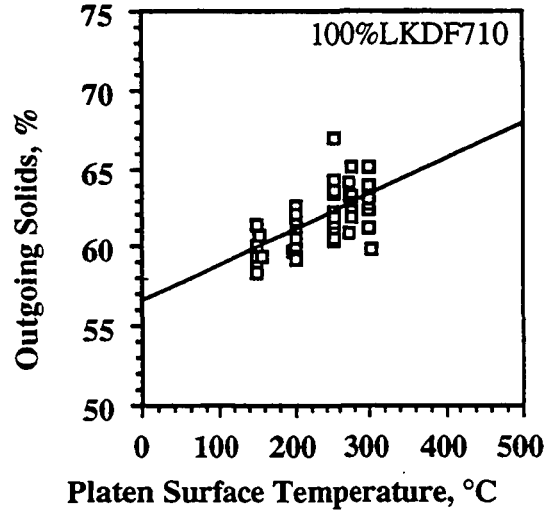


Figure A32. Outgoing solids vs. initial platen surface temperature for impulse drying of 100%LKDF710.

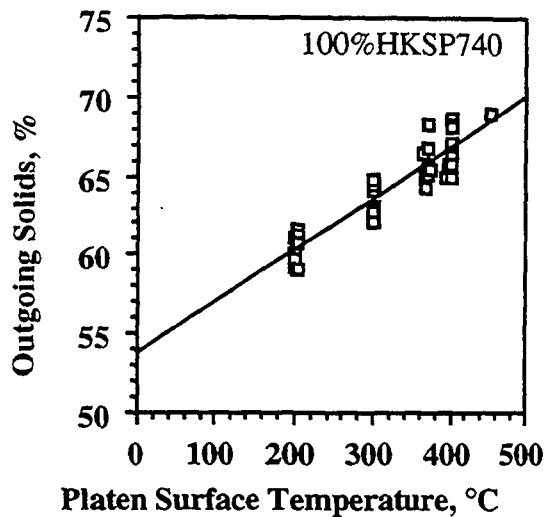


Figure A33. Outgoing solids vs. initial platen surface temperature for impulse drying of 100%HKSP740.

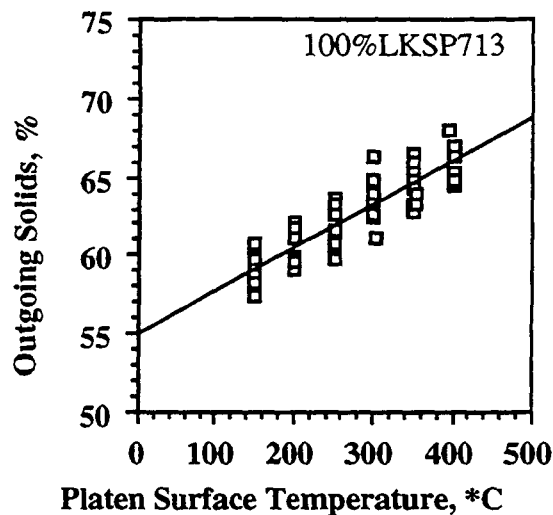


Figure A34. Outgoing solids vs. initial platen surface temperature for impulse drying of 100%LKSP713.

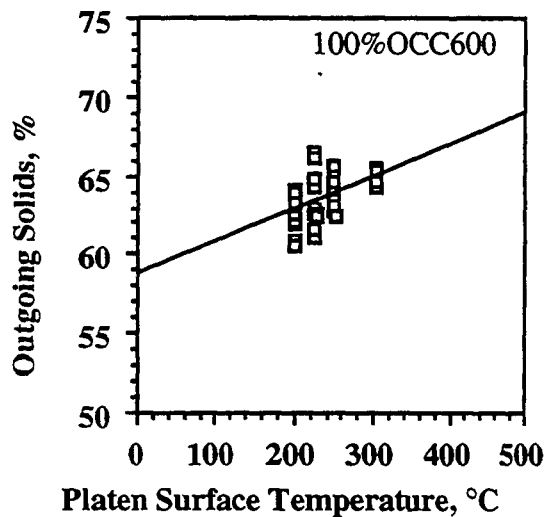


Figure A35. Outgoing solids vs. initial platen surface temperature for impulse drying of 100%OCC600.

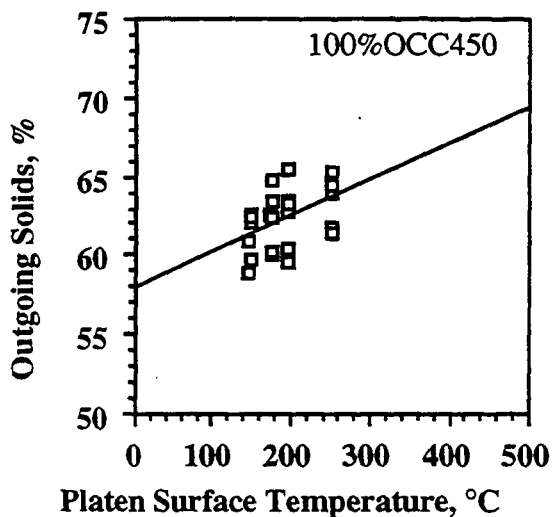


Figure A36. Outgoing solids vs. initial platen surface temperature for impulse drying of 100%OCC450.

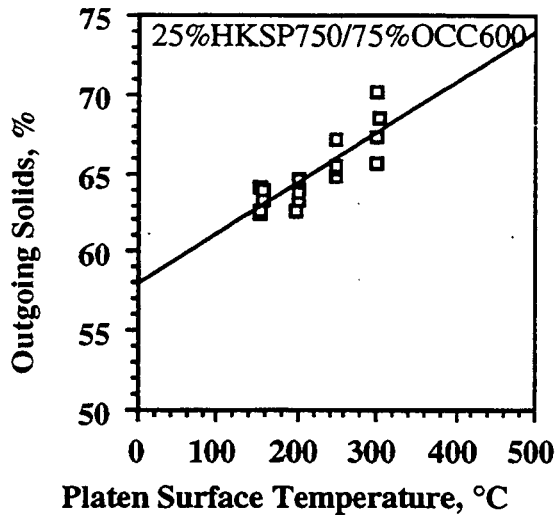


Figure A37. Outgoing solids vs. initial platen surface temperature for impulse drying of 25%HKSP750/75%OCC600.

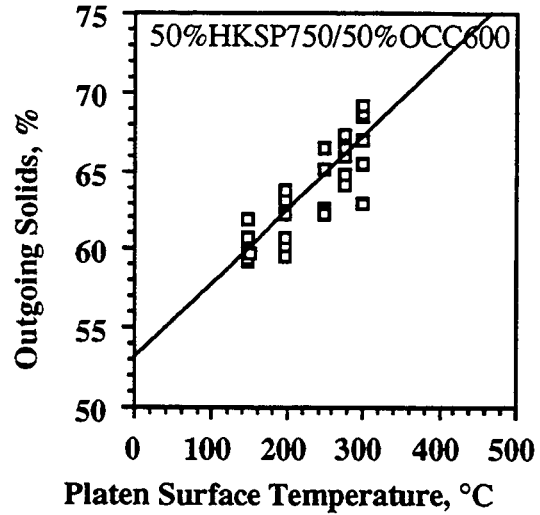


Figure A38. Outgoing solids vs. initial platen surface temperature for impulse drying of 50%HKSP750/50%OCC600.

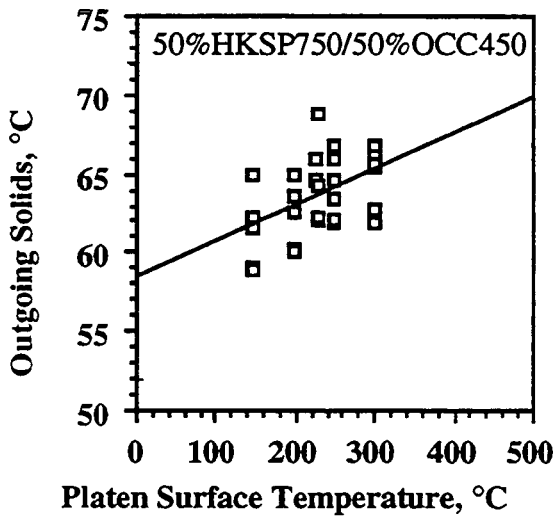


Figure A39. Outgoing solids vs. initial platen surface temperature for impulse drying of 50%HKSP750/50%OCC450.

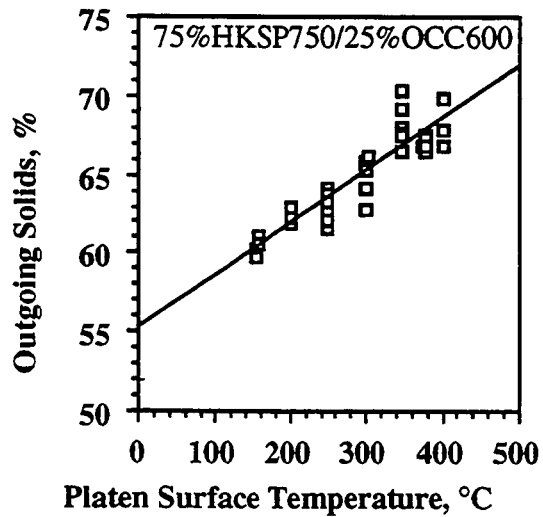


Figure A40. Outgoing solids vs. initial platen surface temperature for impulse drying of 75%HKSP750/25%OCC600.

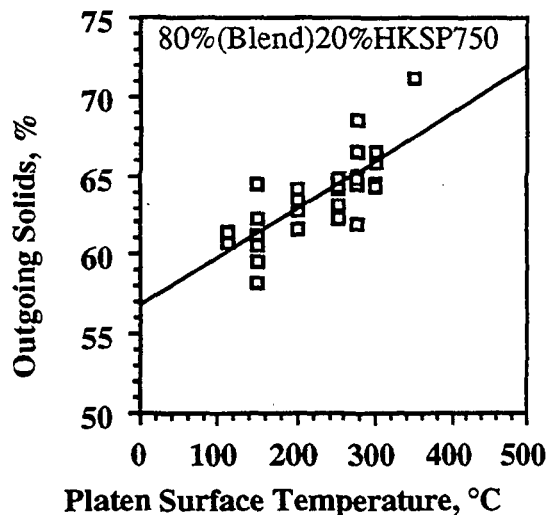


Figure A41. Outgoing solids vs. initial platen surface temperature for impulse drying of 80%(Blend)20%HKSP750.

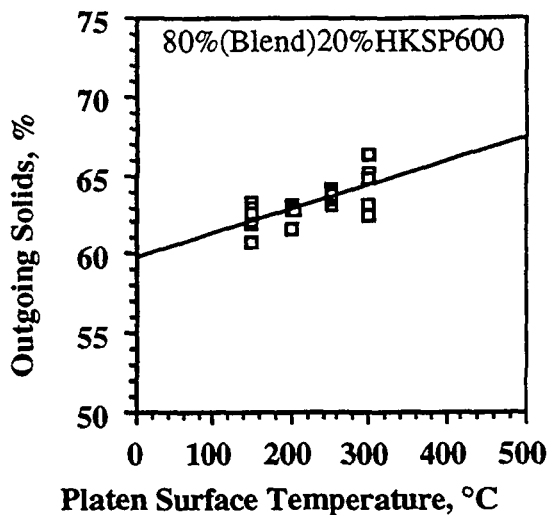


Figure A42. Outgoing solids vs. initial platen surface temperature for impulse drying of 80%(Blend)20%HKSP600.

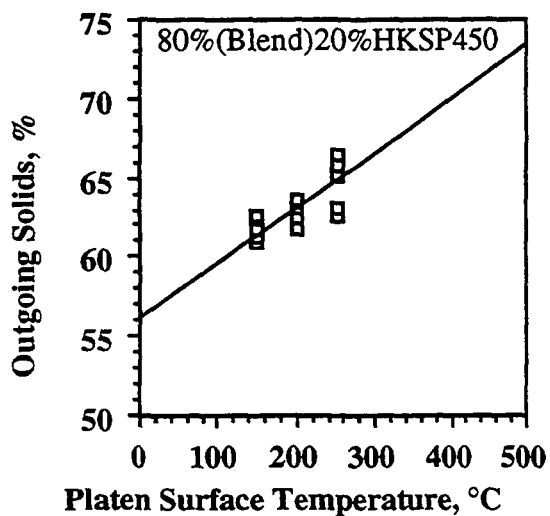


Figure A43. Outgoing solids vs. initial platen surface temperature for impulse drying of 80%(Blend)20%HKSP450.

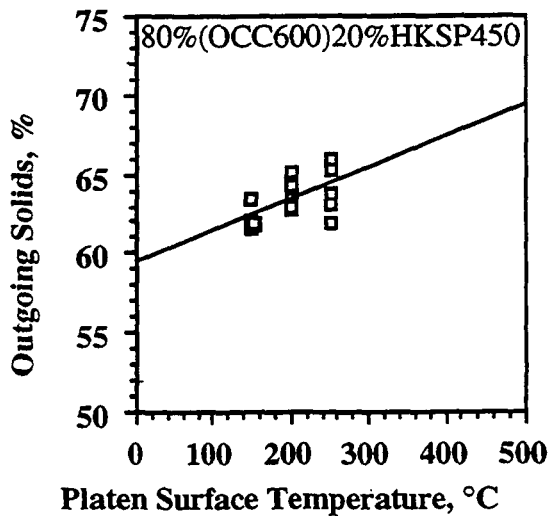


Figure A44. Outgoing solids vs. initial platen surface temperature for impulse drying of 80%(OCC600)20%HKSP450.

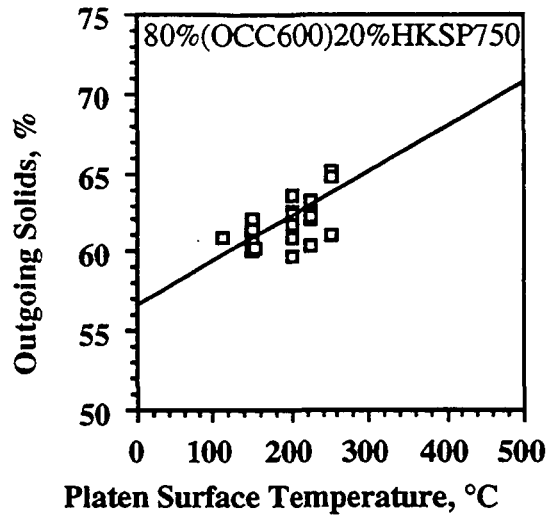


Figure A45. Outgoing solids vs. initial platen surface temperature for impulse drying of 80%(OCC600)20%HKSP750.

**STFI Index vs. Initial Platen Surface Temperature**

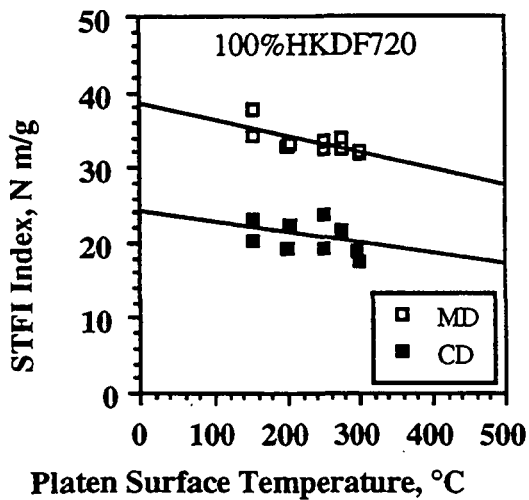


Figure A46. STFI Index vs. initial platen surface temperature for impulse drying of 100%HKDf720.

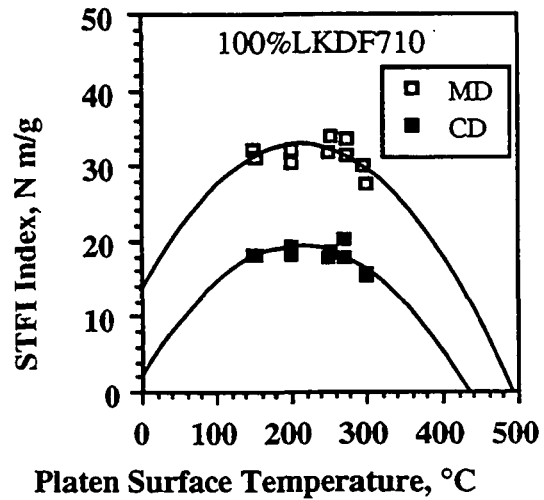


Figure A47. STFI Index vs. initial platen surface temperature for impulse drying of 100%LKDF710.

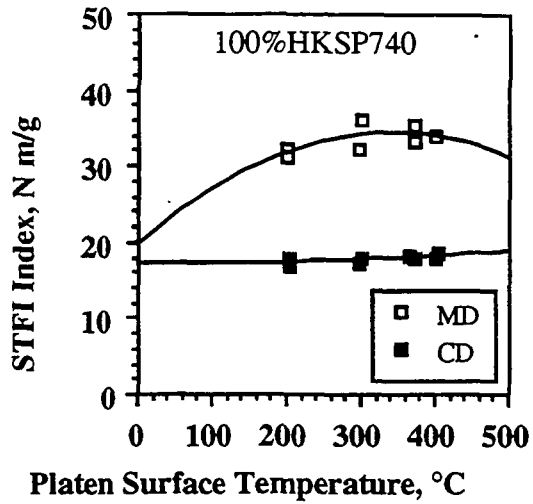


Figure A48. STFI Index vs. initial platen surface temperature for impulse drying of 100%LKSP713.

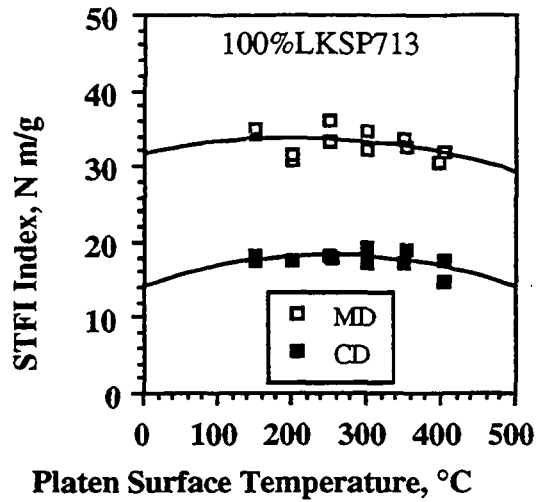


Figure A49. STFI Index vs. initial platen surface temperature for impulse drying of 100%LKSP713.

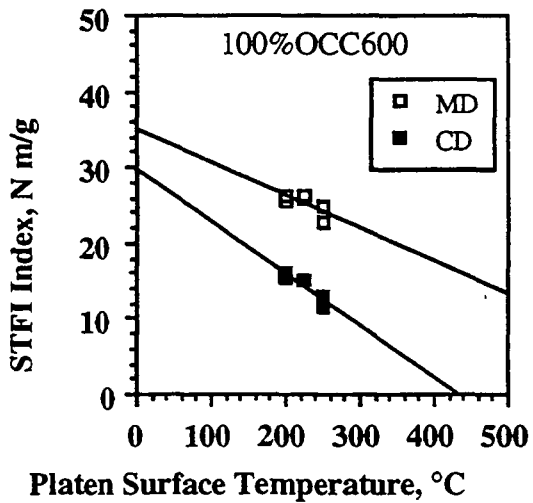


Figure A50. STFI Index vs. initial platen surface temperature for impulse drying of 100%OCC600.

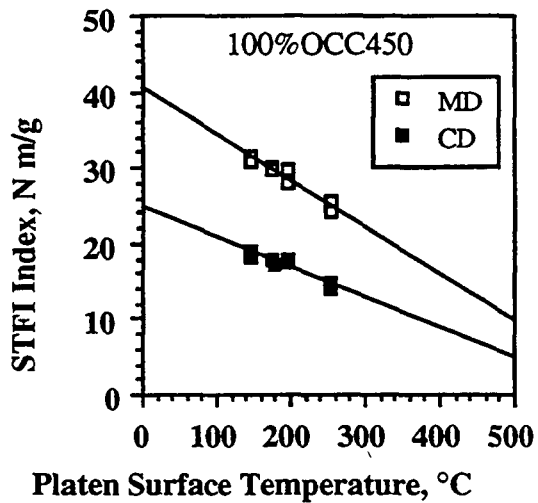


Figure A51. STFI Index vs. initial platen surface temperature for impulse drying of 100%OCC450.

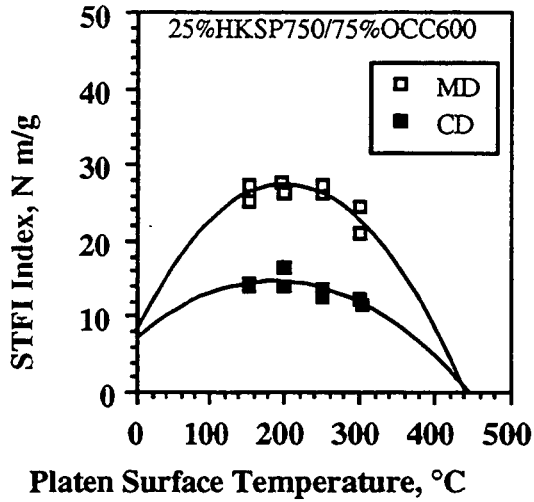


Figure A52. STFI Index vs. initial platen surface temperature for impulse drying of 25%HKSP750/75%OCC600.

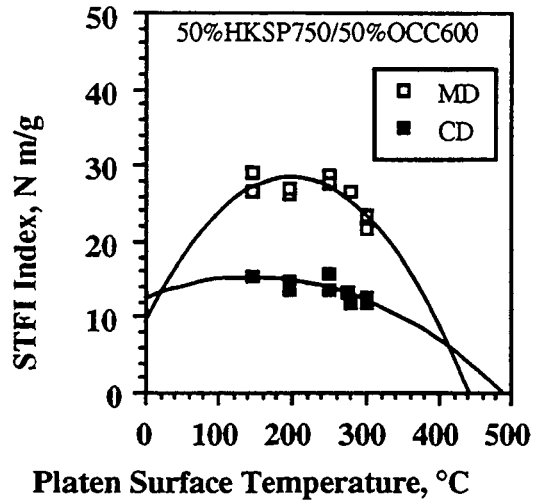


Figure A53. STFI Index vs. initial platen surface temperature for impulse drying of 50%HKSP750/50%OCC600.

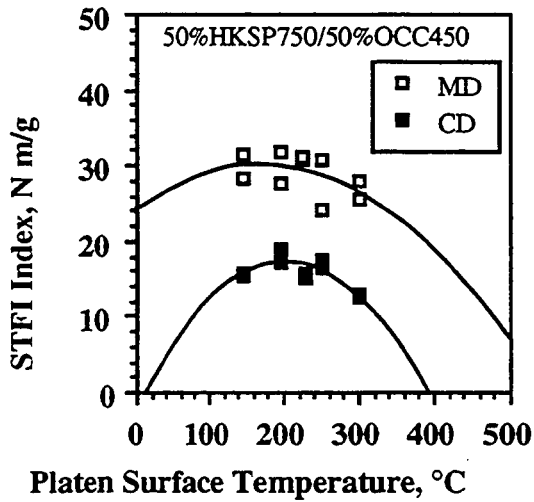


Figure A54. STFI Index vs. initial platen surface temperature for impulse drying of 50%HKSP750/50%OCC450.

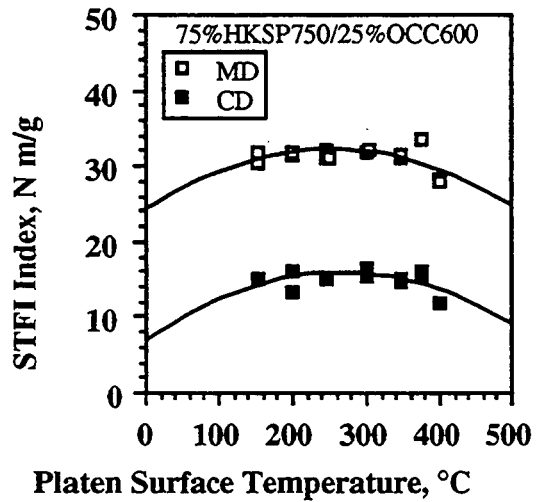


Figure A55. STFI Index vs. initial platen surface temperature for impulse drying of 75%HKSP750/25%OCC600.

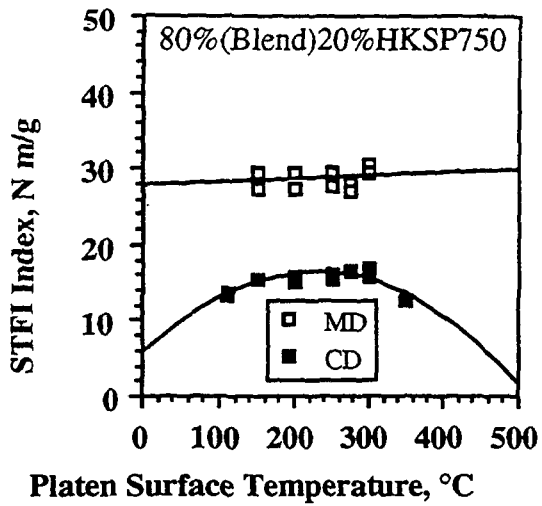


Figure A56. STFI Index vs. initial platen surface temperature for impulse drying of 80%(Blend)20%HKSP750.

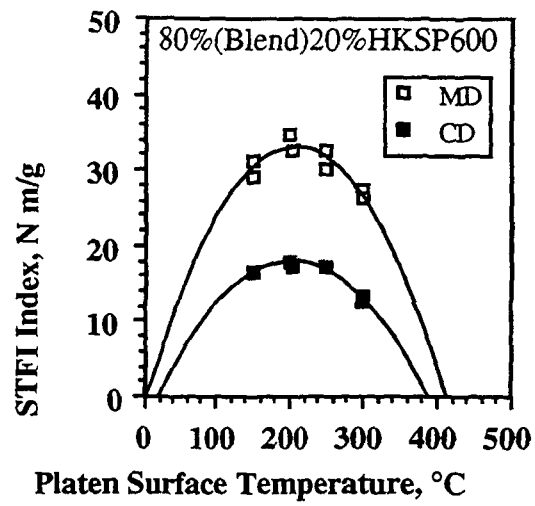


Figure A57. STFI Index vs. initial platen surface temperature for impulse drying of 80%(Blend)20%HKSP600.

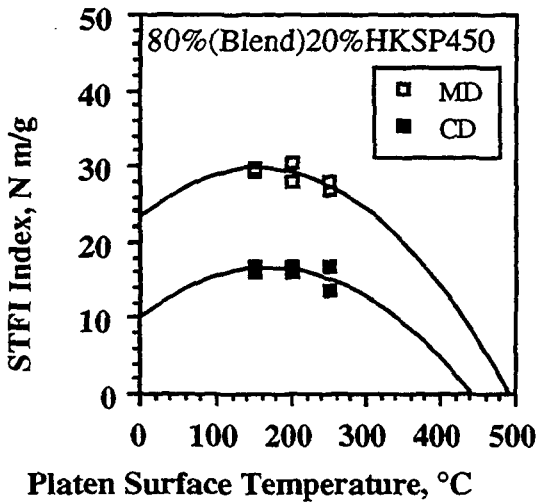


Figure A58. STFI Index vs. initial platen surface temperature for impulse drying of 80%(Blend)20%HKSP450.

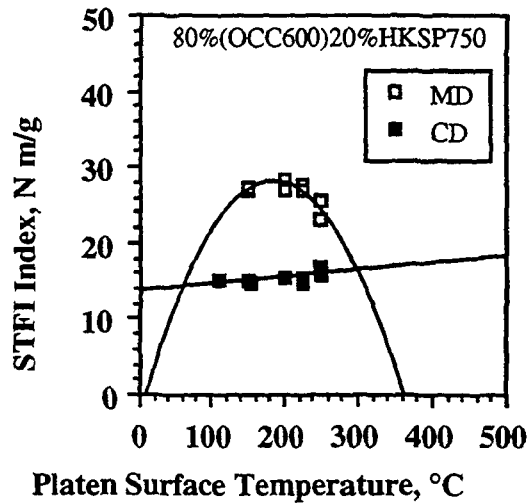


Figure A59. STFI Index vs. initial platen surface temperature for impulse drying of 80%(OCC600)20%HKSP750.

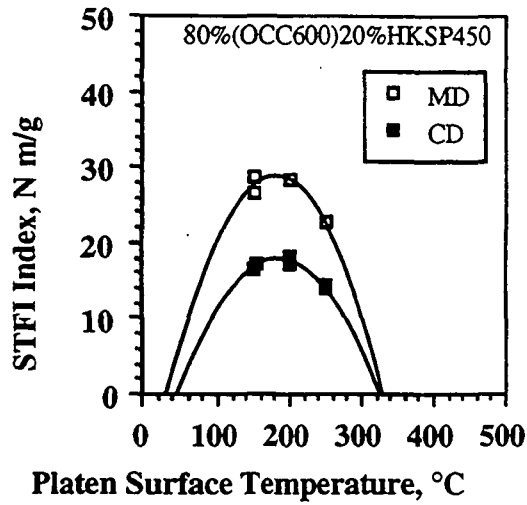


Figure A60. STFI Index vs. initial platen surface temperature for impulse drying of 80%(OCC600)20%HKSP450.

**Density vs. Initial Platen Surface Temperature**

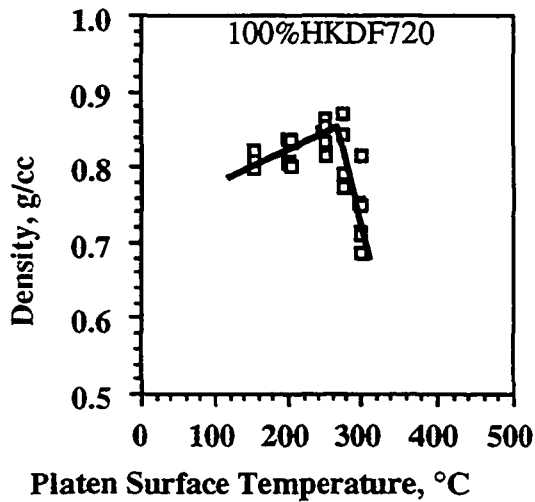


Figure A61. Density vs. initial platen surface temperature for impulse drying of 100%HKDF720.

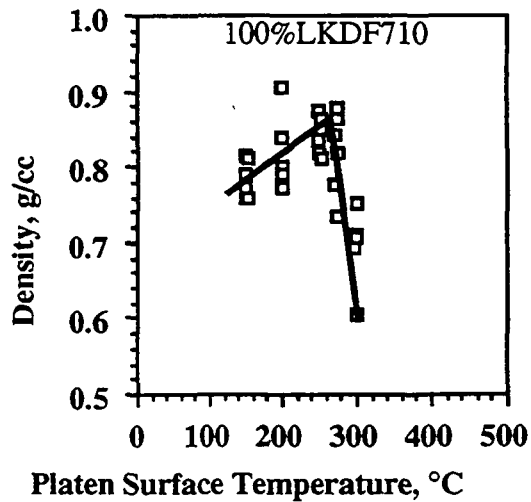


Figure A62. Density vs. initial platen surface temperature for impulse drying of 100%LKDF710.

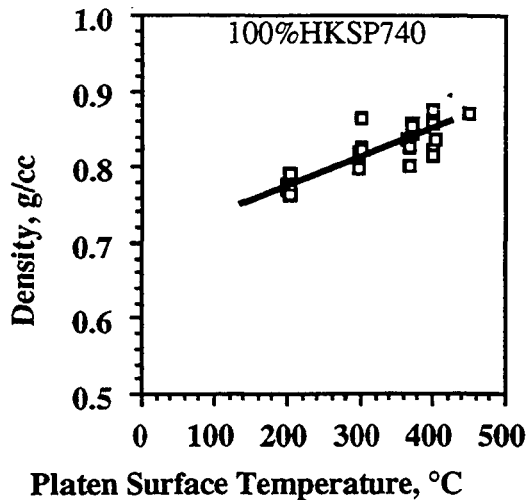


Figure A63. STFI Density vs. initial platen surface temperature for impulse drying of 100%HKSP740.

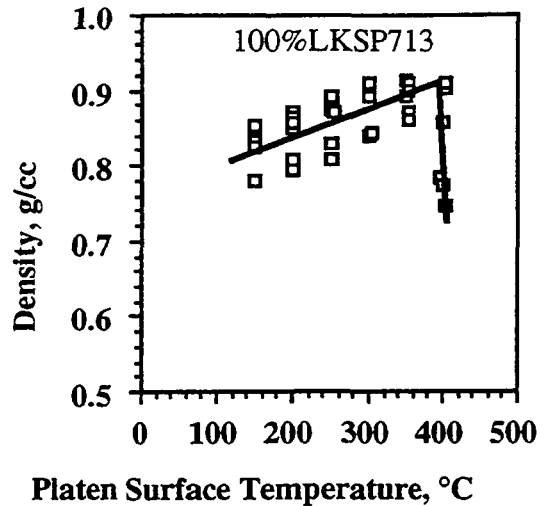


Figure A64. Density vs. initial platen surface temperature for impulse drying of 100%LKSP713.

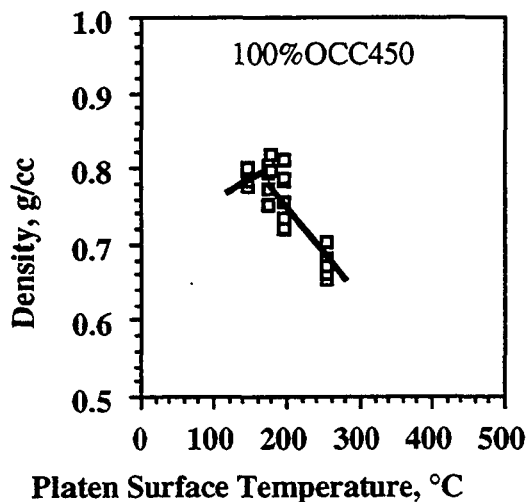


Figure A65. Density vs. initial platen surface temperature for impulse drying of 100%OCC450.

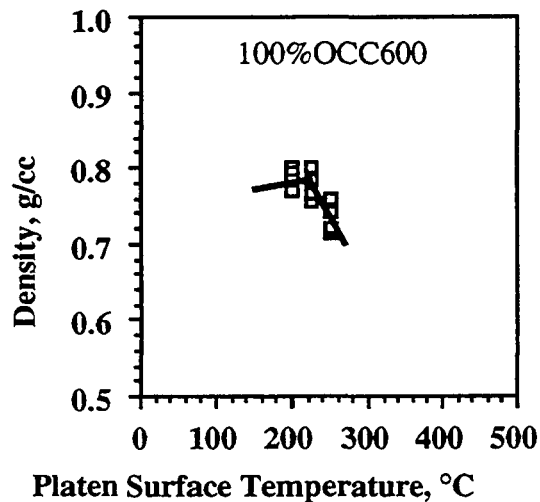


Figure A66. Density vs. initial platen surface temperature for impulse drying of 100%OCC600.

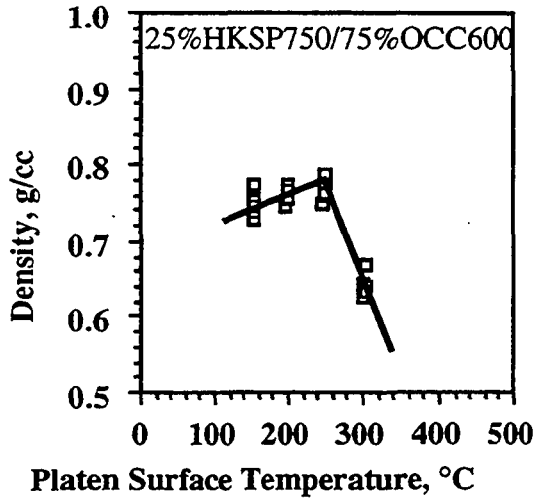


Figure A67. Density vs. initial platen surface temperature for impulse drying of 25%HKSP750/75%OCC600.

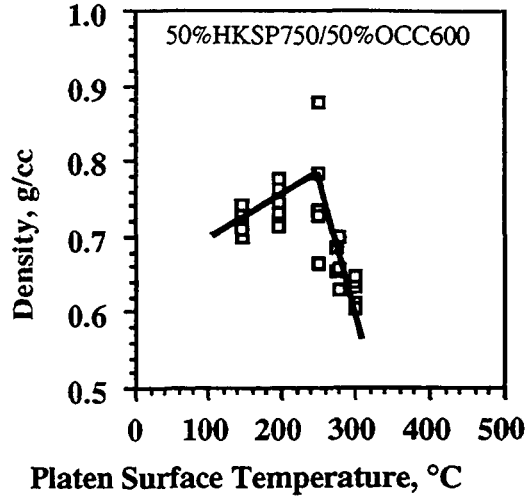


Figure A68. Density vs. initial platen surface temperature for impulse drying of 50%HKSP750/50%OCC600.

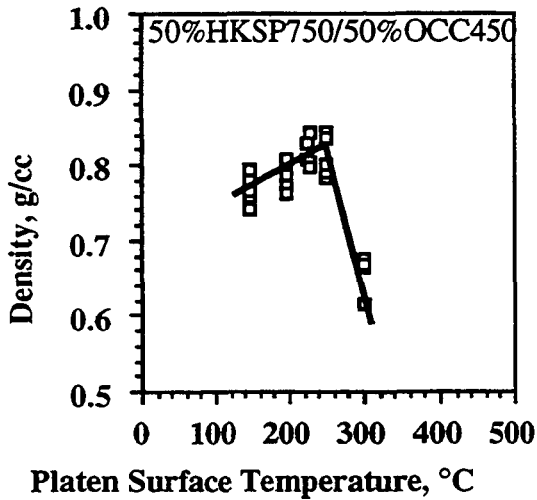


Figure A69. Density vs. initial platen surface temperature for impulse drying of 50%HKSP750/50%OCC450.

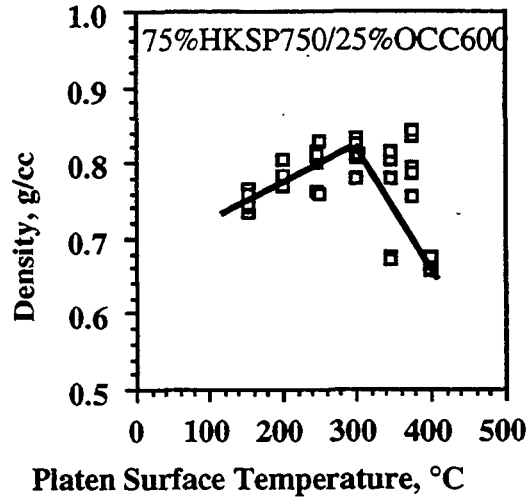


Figure A70. Density vs. initial platen surface temperature for impulse drying of 75%HKSP750/25%OCC600.

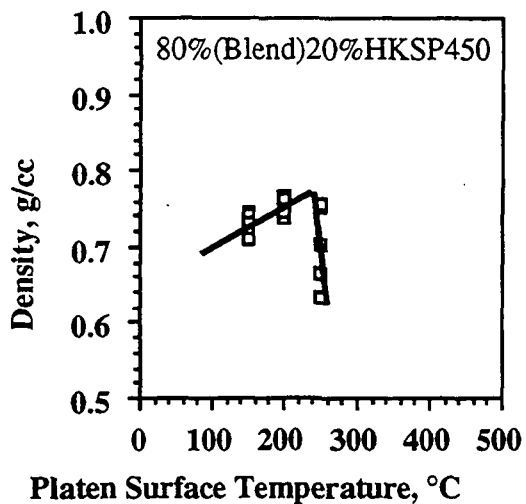


Figure A71. Density vs. initial platen surface temperature for impulse drying of 80%(Blend)20%HKSP450.

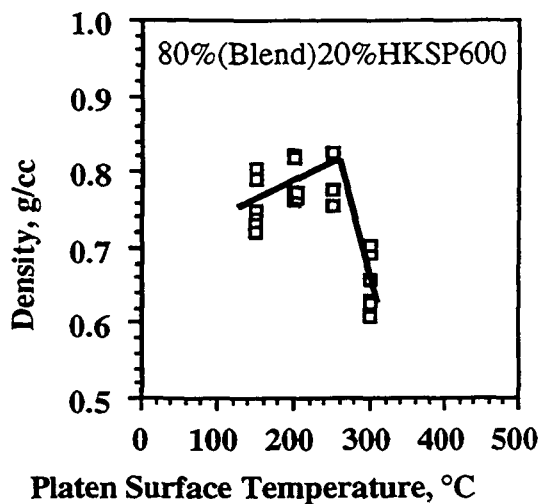


Figure A72. Density vs. initial platen surface temperature for impulse drying of 80%(Blend)20%HKSP600.

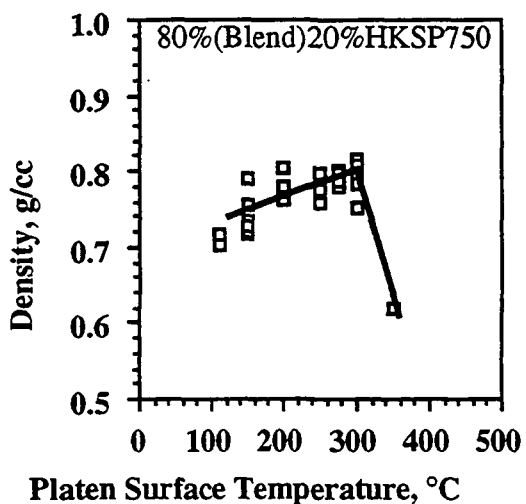


Figure A73. Density vs. initial platen surface temperature for impulse drying of 80%(Blend)20%HKSP750.

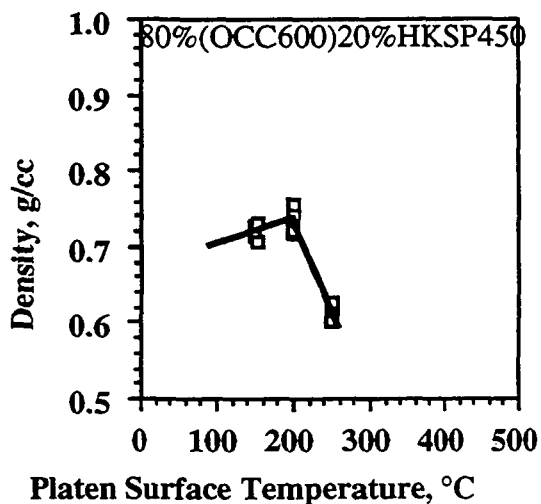


Figure A74. Density vs. initial platen surface temperature for impulse drying of 80%(OCC600)20%HKSP450.

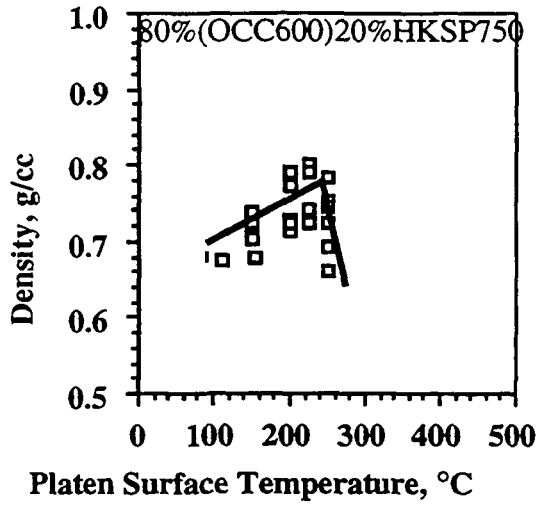


Figure A75. Density vs. initial platen surface temperature for impulse drying of 80%(OCC600)20%HKSP750.

**Burst Index vs. Initial Platen Surface Temperature**

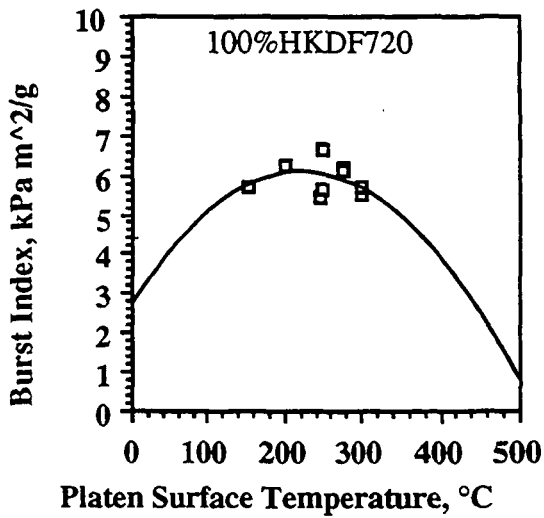


Figure A76. Burst Index vs. initial platen surface temperature for impulse drying of 100%HKDF720.

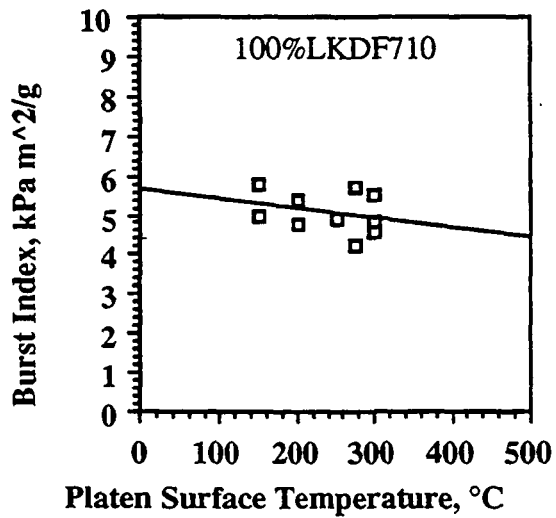


Figure A77. Burst Index vs. initial platen surface temperature for impulse drying of 100%LKDF710.

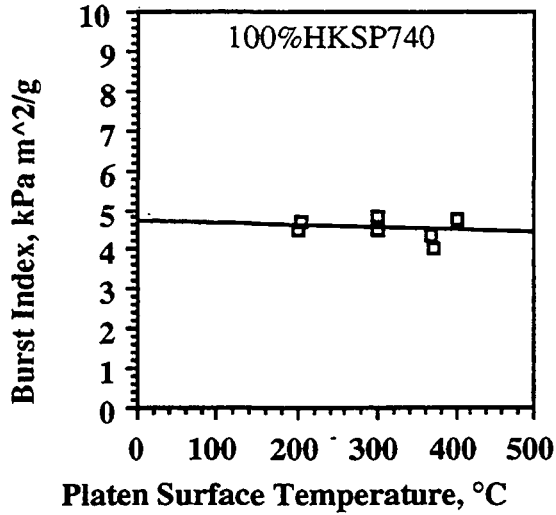


Figure A78. Burst Index vs. initial platen surface temperature for impulse drying of 100%HKSP740.

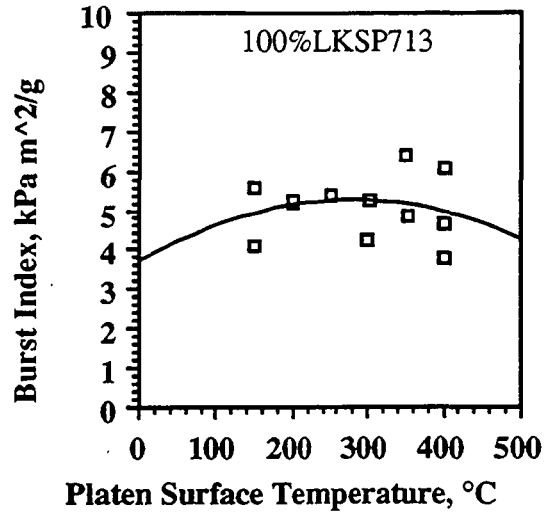


Figure A79. Burst Index vs. initial platen surface temperature for impulse drying of 100%LKSP713.

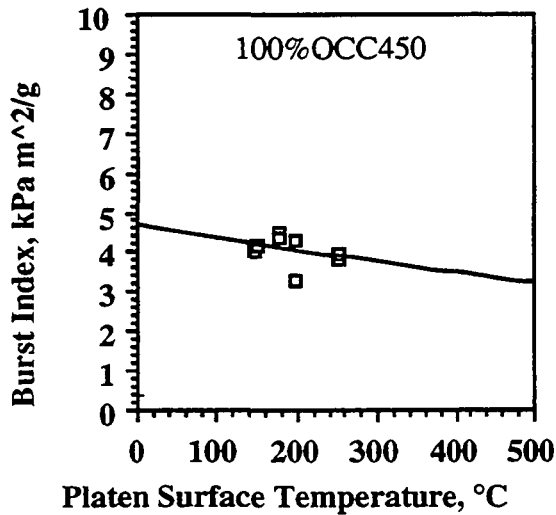


Figure A80. Burst Index vs. initial platen surface temperature for impulse drying of 100%OCC450.

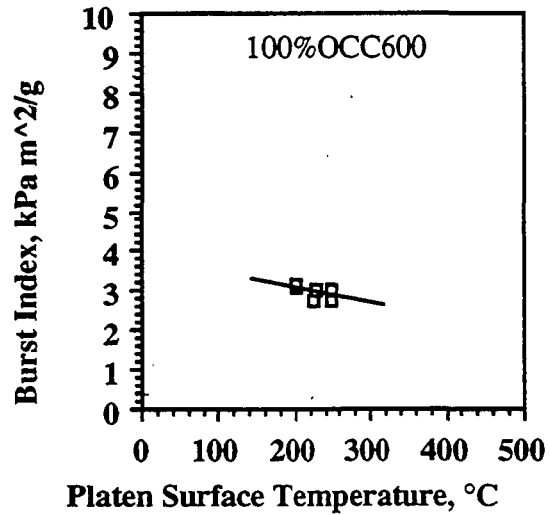


Figure A81. Burst Index vs. initial platen surface temperature for impulse drying of 100%OCC600.

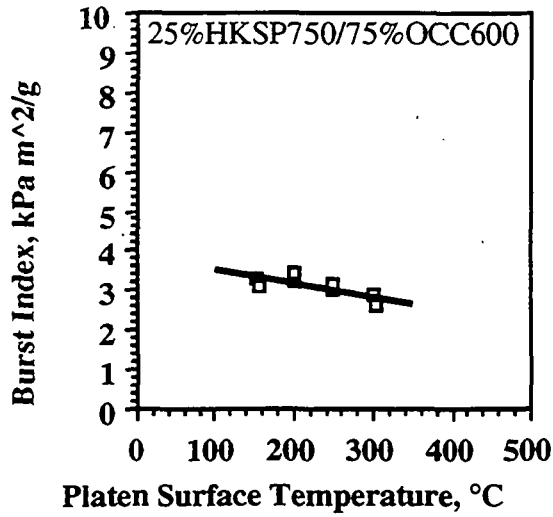


Figure A82. Burst Index vs. initial platen surface temperature for impulse drying of 25%HKSP750/75%OCC600.

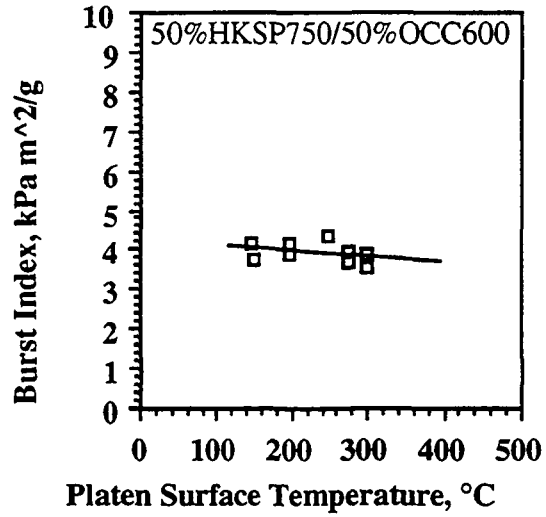


Figure A83. Burst Index vs. initial platen surface temperature for impulse drying of 50%HKSP750/50%OCC600.

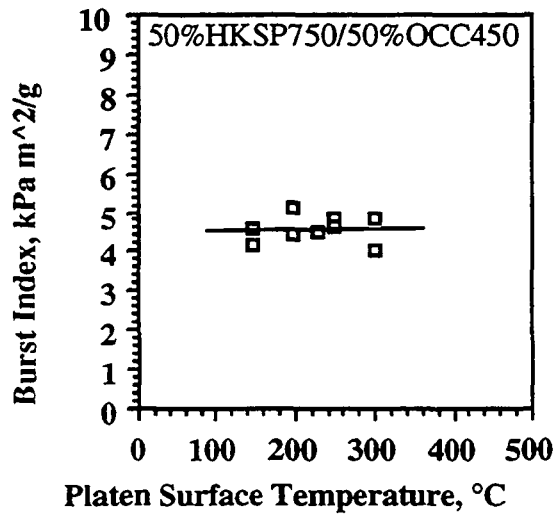


Figure A84. Burst Index vs. initial platen surface temperature for impulse drying of 50%HKSP750/50%OCC450.

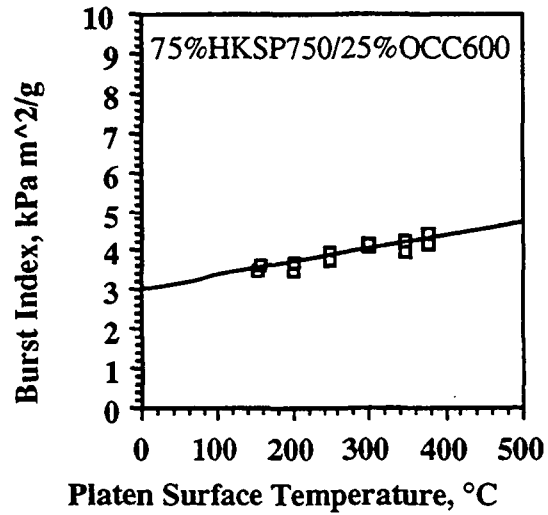


Figure A85. Burst Index vs. initial platen surface temperature for impulse drying of 75%HKSP750/25%OCC600.

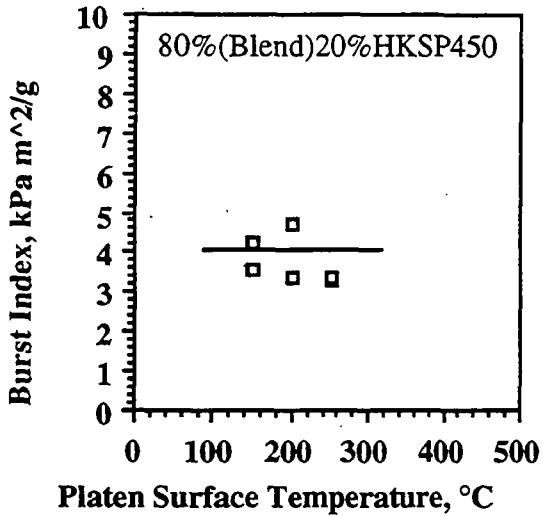


Figure A86. Burst Index vs. initial platen surface temperature for impulse drying of 80%(Blend)20%HKSP450.

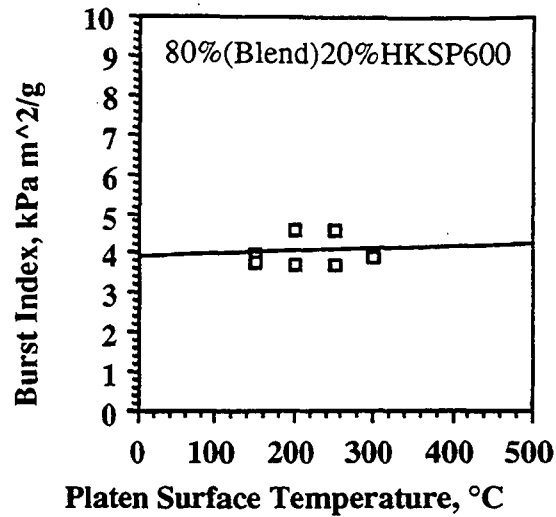


Figure A87. Burst Index vs. initial platen surface temperature for impulse drying of 80%(Blend)20%HKSP600.

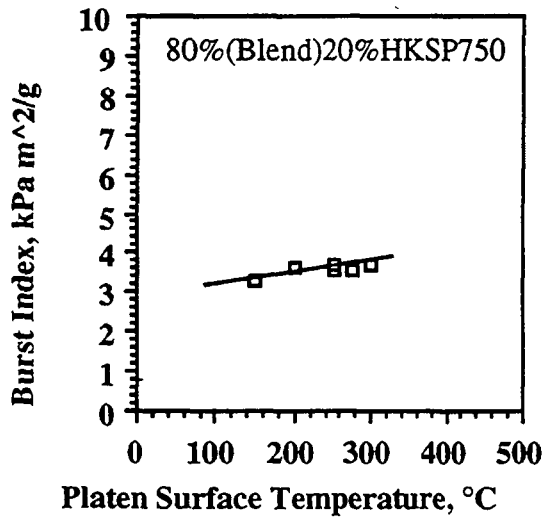


Figure A88. Burst Index vs. initial platen surface temperature for impulse drying of 80%(Blend)20%HKSP750.

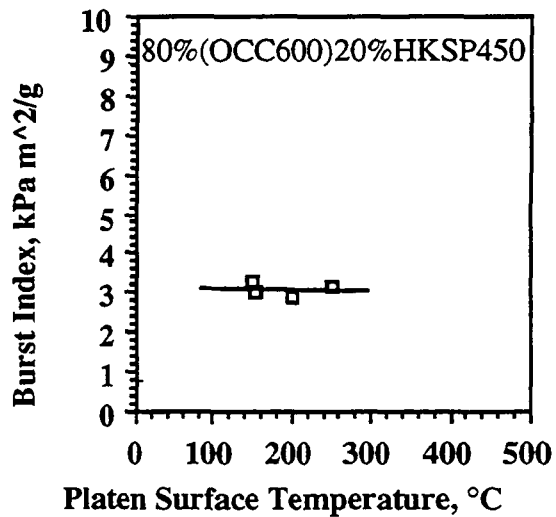


Figure A89. Burst Index vs. initial platen surface temperature for impulse drying of 80%(OCC600)20%HKSP450.

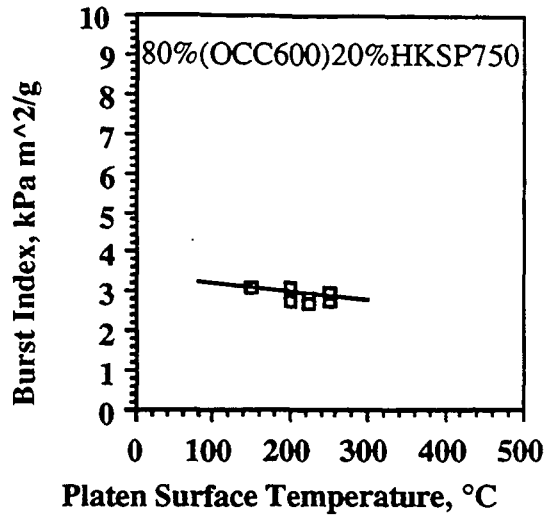


Figure A90. Burst Index vs. initial platen surface temperature for impulse drying of 80%(OCC600)20%HKSP750.

APPROVED: *David I. Orloff*  
 David I. Orloff, Ph.D.  
 Professor of Engineering and  
 Acting Director Engineering and Paper Materials Division

IPST HASLTON LIBRARY



5 0602 01056575 4